Journal of Sedimentary Research

Journal of Sedimentary Research, 2015, v. 85, 489–508
Research Article
DOI: http://dx.doi.org/10.2110/jsr.2015.31

PLANKTONIC FORAMINIFERAL BIOSTRATIGRAPHY, MICROFACIES ANALYSIS, SEQUENCE STRATIGRAPHY, AND SEA-LEVEL CHANGES ACROSS THE CRETACEOUS–PALEOGENE BOUNDARY IN THE HAYMANA BASIN, CENTRAL ANATOLIA, TURKEY

SELEN ESMERAY-SENLET,[1] SEVİNÇ ÖZKAN-ALTINER,[2] DEMİR ALTINER,[2] AND KENNETH G. MILLER[1]
[1]*Department of Earth and Planetary Sciences, Rutgers University, Piscataway, New Jersey 08854, U.S.A.*
[2]*Department of Geological Engineering, Middle East Technical University, 06531 Ankara, Turkey*
e-mail: esmeray@rutgers.edu

ABSTRACT: **The Cretaceous–Paleogene (K/Pg) boundary in the Haymana Basin, Central Anatolia, Turkey, was delineated using planktonic foraminiferal biostratigraphy, microfacies analysis, and sequence stratigraphy. An ~ 29 m outcrop consisting of limestone and marl was measured, and four planktonic foraminiferal biozones were identified spanning the boundary. Planktonic foraminiferal extinction across the K/Pg boundary was catastrophic and abrupt. The extinction level is overlain by a unit (Zone P0) showing an increase in echinoid fecal pellets and authigenic clay minerals such as glauconite, suggesting low sedimentation rates in the early Danian. Ten microfacies types were identified indicating inner-ramp to basinal paleoenvironments based on the sedimentological characteristics and microfossil and macrofossil assemblages. Maastrichtian carbonates contain large benthic foraminifera, calcareous red algae, bryozoans, fragments of echinoderms and mollusks, and planktonic foraminifera. Overlying Maastrichtian–Danian silty marls and silty limestones have common planktonic and benthic foraminifera. Progradation of carbonates into the basin took place during the highstand systems tract, and deposition of a silty marl succession occurred during the transgressive systems tract. The K/Pg boundary is in the upper part of the transgressive systems tract, below a maximum flooding surface. Sequence stratigraphic analysis of a second section, Campo Pit, New Jersey, USA, showed that the K/Pg boundary occurs within a transgressive systems tract in New Jersey as well, suggesting a global sea-level rise across the K/Pg boundary.**

INTRODUCTION

The Cretaceous–Paleogene (K/Pg) boundary denotes one of the five largest mass extinctions in Earth history (Raup and Sepkoski 1982), where a number of major groups disappeared, such as nonavian dinosaurs, marine and flying reptiles, ammonites, and rudists (Schulte et al. 2010 and the references therein). In the marine realm, the turnover of calcareous nannofossils and planktonic foraminifera was especially remarkable (e.g., Bernaola and Monechi 2007; Olsson and Liu 1993). More than 90% of Cretaceous planktonic foraminifera became extinct at the K/Pg boundary with three survivor species, *Guembelitria cretacea*, *Hedbergella holmdelensis*, and *Hedbergella monmouthensis*, giving rise to the evolution of all Paleogene planktonic foraminifera (Olsson and Liu 1993; Olsson et al. 1999).

The global stratotype section of the K/Pg boundary at El-Kef, Tunisia, is characterized by a boundary clay, an Ir anomaly, and an increase in Ni-rich spinels (Ben Abdelkader et al. 1997). The presence of microtektites and shocked quartz is another important characteristic of K/Pg boundary sections in various locations in the world (Smit 1999). However, none of these lithological or geochemical criteria alone is enough to identify the boundary, and paleontological evidence is needed. The extinction level of Cretaceous planktonic foraminifera is a global horizon that is used for the correlation of the K/Pg boundary in marine sections worldwide (e.g., Luterbacher and Premoli Silva 1964; Olsson and Liu 1993; Olsson et al. 1999).

The objective of this study is to delineate the K/Pg boundary in the Haymana Basin (Fig. 1), a sedimentary basin in Central Anatolia, Turkey, using planktonic foraminiferal biostratigraphy, determine the depositional history of the basin with a comprehensive microfacies analysis, and place the section within a sequence stratigraphic framework. We also aim to develop a relative sea-level curve for the Haymana Basin and compare it with sections elsewhere, including new data from New Jersey, USA. In spite of numerous studies, there is still no consensus on the global sea-level changes across the K/Pg boundary (e.g., Claeys et al. 2002). Detailed microfacies analysis of the Haymana Basin and the stratigraphic comparison with sections in other geographic locations will help us to understand the global sea-level changes across the boundary. Understanding the depositional history and paleontologic characteristics of the Haymana Basin will be useful in future exploration of similar basins, and will help us to elucidate global aspects of the K/Pg boundary.

GEOLOGICAL SETTING

The Haymana Basin, situated in Central Anatolia, is a forearc basin formed during the Late Cretaceous to late Eocene on the oceanic crust of the northern branch of Neo-Tethys (i.e., Izmir–Ankara suture zone, Fig. 1A). It was formed by the convergence and collision of the Eurasian plate to the north, the Gondwana plate to the south, and the adjacent Sakarya continent (Fourquin 1975; Şengör and Yılmaz 1981; Görür et al.

Published Online: May 2015
 1527-1404/15/085-489/$03.00

1984; Koçyiğit 1991; Koçyiğit et al. 1998). The basin is surrounded by the Sakarya continent to the north-northwest, the metamorphic Kırşehir massif to the east, and the Menderes–Taurid block to the south (Fig. 1A).

The existence of the calc-alkaline Galatean volcanics in the Pontides during the Paleogene and the ophiolitic basement show that the basin was developed on an accretionary wedge, which was active from the Late Cretaceous to the late Eocene (Şengör and Yılmaz 1981; Görür et al. 1984; Koçyiğit 1991). The arc activity in the Sakarya continent shows that the subduction was towards to the north (Fourquin 1975; Şengör and Yılmaz 1981), and the deformation in the basin continued until the late Pliocene (Koçyiğit 1991).

The Haymana Basin consists of highly deformed and continuous Maastrichtian to upper Eocene sedimentary fill that is greater than 5 km thick (Ünalan et al. 1976; Görür 1981). Deposition was dominated mostly by deep-marine flysch. The center of the basin consists mainly of turbidites, whereas towards the margins there are platform carbonates, continental red beds, and reefal buildups with some volcanic intercalations (Yüksel 1970; Görür 1981; Koçyiğit and Lünel 1987; Çiner 1992). Our measured section represents the K/Pg transition in the Beyobasi Formation, which overlies shales of the Haymana Formation and underlies the limestones of Çaldağ Formation (Ünalan et al. 1976). It consists of shelf to basin limestones and marls and is located approximately 10 km southwest of the town of Haymana, which is situated 70 km southwest of Ankara, Turkey (Fig. 1B). Previous biostratigraphic studies indicated that the K/Pg boundary is conformable in the study area (Özkan-Altıner and Özcan 1999).

METHODS AND MATERIALS

A 29.41-m-thick section was measured in the Haymana Basin consisting of marls and limestones, and 90 samples were collected throughout the section for biostratigraphic, lithostratigraphic, and microfacies analysis. Sixty samples (A1–A60) were collected from the section with a sampling interval of 10–100 cm (Fig. 2). In order to sample the lowest occurrences of the earliest Danian forms and to be able to construct a detailed planktonic foraminiferal biozonation across the boundary, a 2.34-m-thick interval of the measured section including the boundary (between samples A48–A54) was trenched, resampled, and 30 additional samples (B1–B30) were collected with a sampling interval of 2–10 cm (Fig. 3).

Because the samples are indurated, several washing techniques were applied for the taxonomic and biostratigraphic studies. Neither conventional planktonic foraminifera washing techniques such as soaking the samples with hydrogen peroxide or acetic acid with different dilutions and durations, nor methods such as Knitter (1979) and Lirer (2000) yielded satisfactory results for limestone samples. Therefore, we developed a specific washing technique in order to obtain foraminiferal specimens. Approximately 25 g of sample was broken down into 2–5 mm^3 pieces and soaked in a 250 ml solution of 50% diluted hydrogen peroxide for marl samples and half composed of 50% diluted hydrogen peroxide and half composed of 50% diluted acetic acid for limestone samples. The mixture was shaken with a magnetic splitter for 45–60 minutes, and then the samples were washed under running water through 425, 250, 125, and 63 μm sieves. In order to facilitate identification, picked samples were ultrasonically cleaned for 4–7 minutes. Thin sections of the samples were prepared in the Department of Geological Engineering, Middle East Technical University, for mineralogical and microfacies analysis.

The taxonomic determinations of planktonic foraminifera are based on Robaszynski et al. (1984), Nederbragt (1991), and Premoli-Silva and Verga (2004) for the Late Cretaceous species and Olsson et al. (1999) for the early Paleogene species. Despite the poor to moderate preservation of the species, key morphological characteristics such as coiling mode, peripheral shape, arrangement and number of the chambers, presence or absence of keels, and sutural properties enabled us to construct a reliable biostratigraphy.

Carbonate rocks in the section were identified based on the Dunham (1962) and Embry and Klovan (1971) classifications of carbonate rocks. For the mixed siliciclastic–carbonate rocks, the principles proposed in the Mount (1985) classification were utilized. Major fossil groups were determined using the descriptions and photographs in Flügel (2004), Scholle and Ulmer-Scholle (2003), and Horowitz and Potter (1971). For the determination of the depositional environments, microfacies models of Wilson (1975) and Flügel (2004) were used.

Microfacies analysis was performed by examining mineralogical components, macrofossil, and microfossil assemblages, and texture of the samples observed in thin sections and outcrop. Rock-forming fossil groups like gastropods, pelecypods, echinoderms, bryozoans, hyaline large and smaller benthic foraminifera, agglutinated benthic foraminifera, and calcareous red and green algae were identified without taxonomic details in thin sections in order to determine the environment of deposition. Furthermore, echinoid fecal pellets from the 63–250 μm size fraction were counted using a micro-splitter, and number of fecal pellets per gram of sample was determined.

A 6-m-thick section was measured at Campo Pit, Perrineville, New Jersey, and 15 samples were collected for lithostratigraphic and sequence stratigraphic analyses. Samples were disintegrated using Calgon solution (5.5 g of sodium metaphosphate per 4 liters of water) and washed with tap water through a 63-μm sieve. Dry weights before and after washing were noted to calculate the sand/mud ratio of the samples. After drying in an oven at 40°C, samples were sieved through 250, 150, 125, and 63 μm sieves and each size fraction was examined separately for mineralogical analysis. Semiquantitative cumulative percentage analysis of minerals was conducted by visual estimation for medium ($>$ 250 μm) and fine ($<$ 250 μm) sand fractions separately.

RESULTS

Lithostratigraphy

The lowermost part of the section (samples A1–A23) consists of yellowish, highly fractured, bioclastic carbonates rich in hyaline and agglutinated benthic foraminifera, calcareous red algae, bryozoans, mollusks, and echinoderm fragments with minor amounts of Late Cretaceous planktonic foraminifera (Fig. 2). Above this ~ 7-m-thick interval of packstone, grainstone, floatstone, and wackestone–packstone alternation, wackestone with planktonic organisms including planktonic foraminifera and calcispheres was deposited in a deeper-water setting (samples A24–A26). Samples A27 and A30 (~ 2 m) are from a quartz-rich silty limestone with Cretaceous ammonites, large benthic foraminifera, calcareous red algae, bryozoans, mollusks, and echinoderm fragments. The overlying unit is an 18-m-thick, dark gray to green silty marl that spans the K/Pg boundary (A30–A52/B17). The number of large benthic foraminifera, algae, mollusks, and echinoderm fragments decreases upsection and the number of planktonic foraminifera, agglutinated, and hyaline benthic foraminifera increases in the silty marl succession. The K/Pg boundary is placed between samples A50–A51

→

FIG. 1.—**A)** Location of the Haymana Basin within the main structural features of Turkey (Koçyiğit 1991; Çiner et al. 1996) **B)** Generalized geological map of the Haymana Basin (modified from 1/500,000 scale Turkey Map). The location of the study area (39° 24′ 20″ N, 32° 27′ 55″ E) is indicated with a black rectangle.

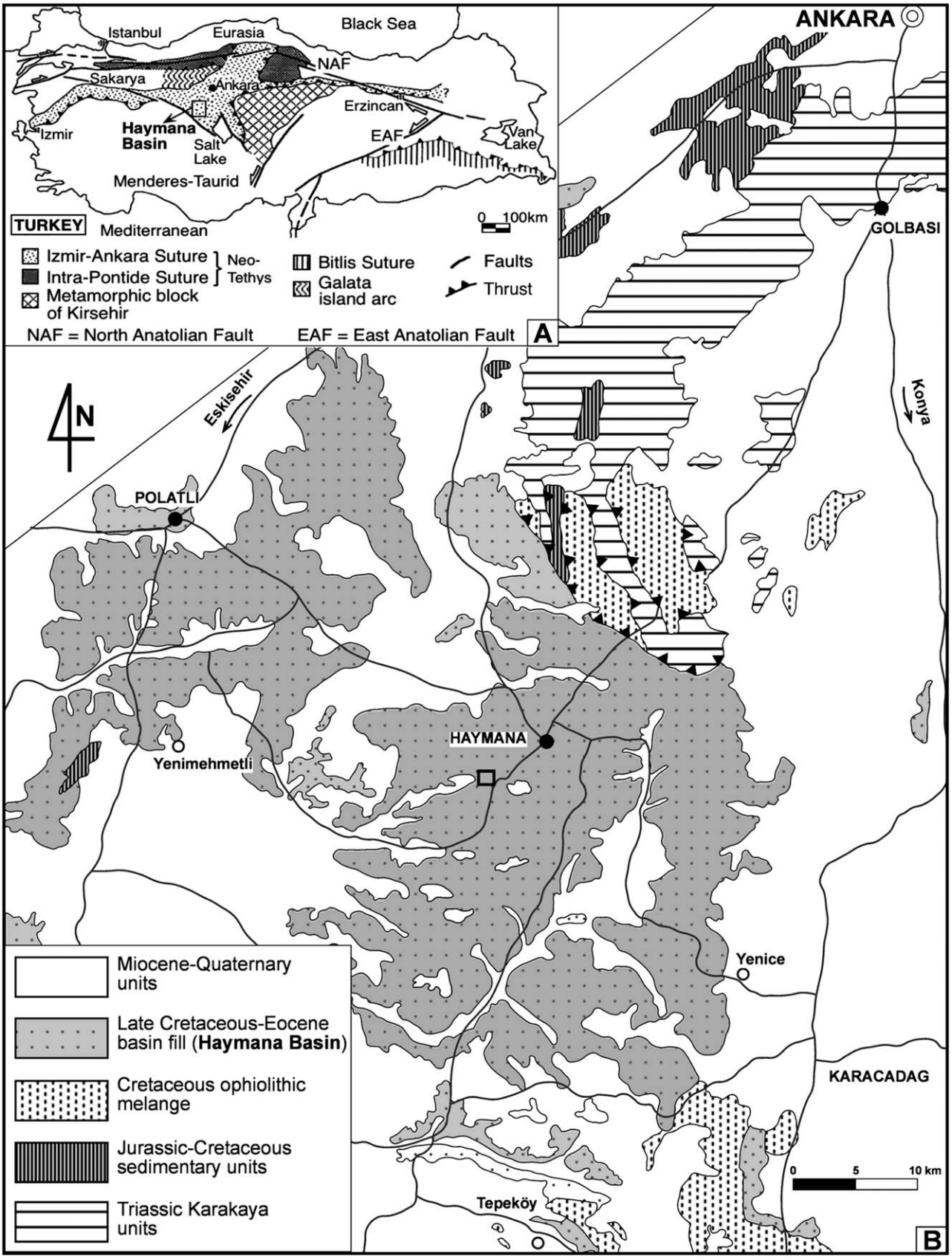
Istanbul
Eurasia
Black Sea
NAF
Sakarya
Ankara
Erzincan
Izmir
Haymana Basin
Salt Lake
EAF
Van Lake
Menderes-Taurid
TURKEY
Mediterranean
0 100km
Izmir-Ankara Suture
Intra-Pontide Suture
Neo-Tethys
Metamorphic block of Kirsehir
Bitlis Suture
Galata island arc
Faults
Thrust
NAF = North Anatolian Fault
EAF = East Anatolian Fault
A
ANKARA
GOLBASI
Konya
Eskisehir
N
POLATLI
Yenimehmetli
HAYMANA
Yenice
KARACADAG
Tepeköy
0 5 10 km
Miocene-Quaternary units
Late Cretaceous-Eocene basin fill (Haymana Basin)
Cretaceous ophiolithic melange
Jurassic-Cretaceous sedimentary units
Triassic Karakaya units
B

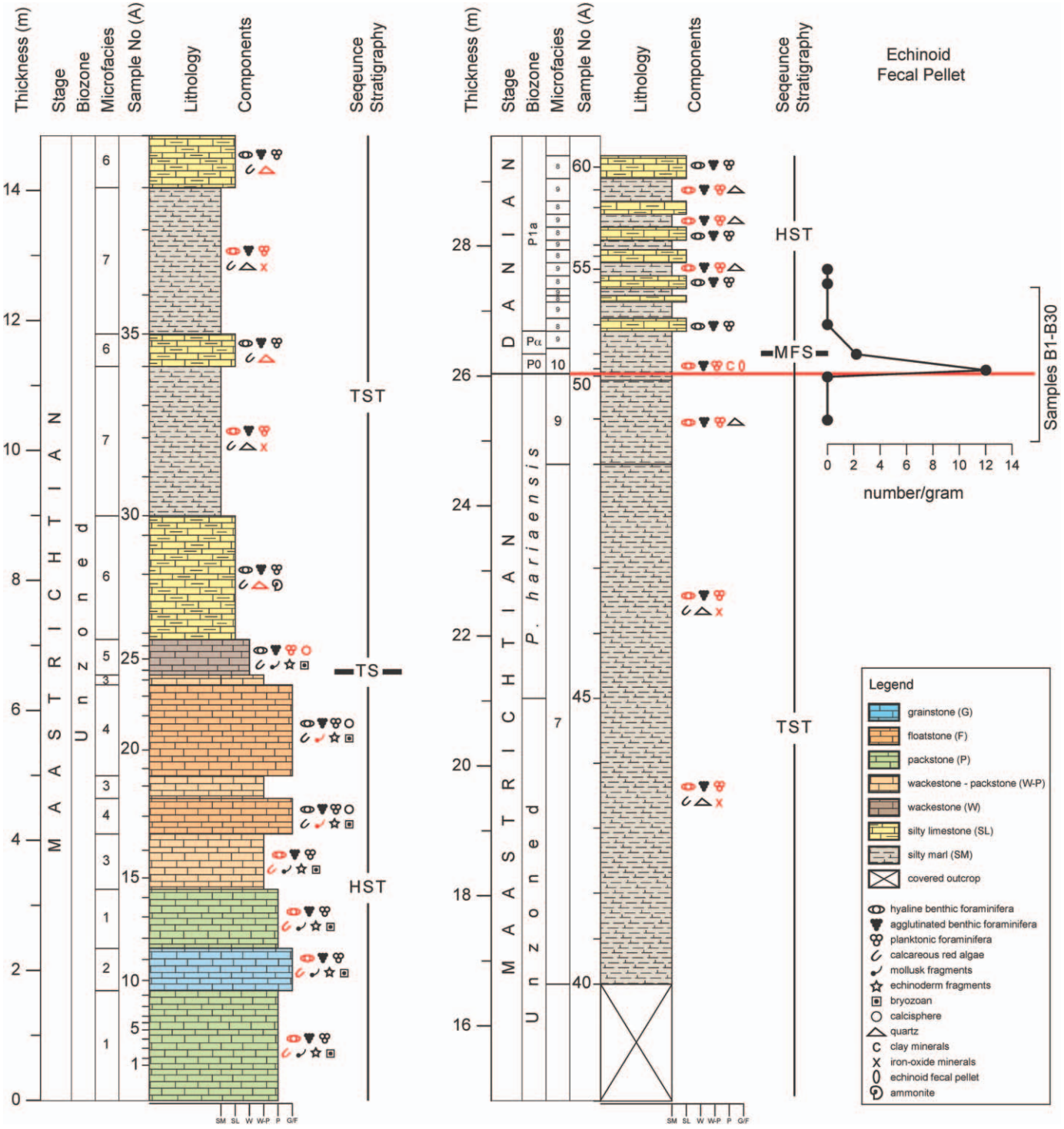

FIG. 2.—Lithostratigraphy, planktonic foraminiferal biozones, microfacies types, sequence stratigraphical interpretation, and echinoid fecal pellet counts of the measured section (samples A1–A60). The most abundant biogenic and abiogenic components are shown in red. Note the stratigraphic level of the detailed section (samples B1–B30) across the boundary, which is shown in Figure 3. HST, highstand systems tract; TST, transgressive systems tract; TS, transgressive surface; MFS, maximum flooding surface.

(B13–B14) upsection, in the transition from the silty marls to the silty marl–silty limestone alternations (Figs. 2, 3). Just above the boundary (B14, B15/A51), a remarkable increase in green clay minerals including glauconite, smectite, chlorite, and echinoid fecal pellets occurs (Figs. 2, 3). In the Danian, silty limestone–silty marl alternations occur above sample A52/B17 up to sample A60 (~ 3 m). Limestones in the uppermost part of the section contain silt and clay and are rich in planktonic and benthic foraminifera.

TABLE 1.—*Distribution of planktonic foraminifera in the Haymana Basin across the K/Pg boundary.*

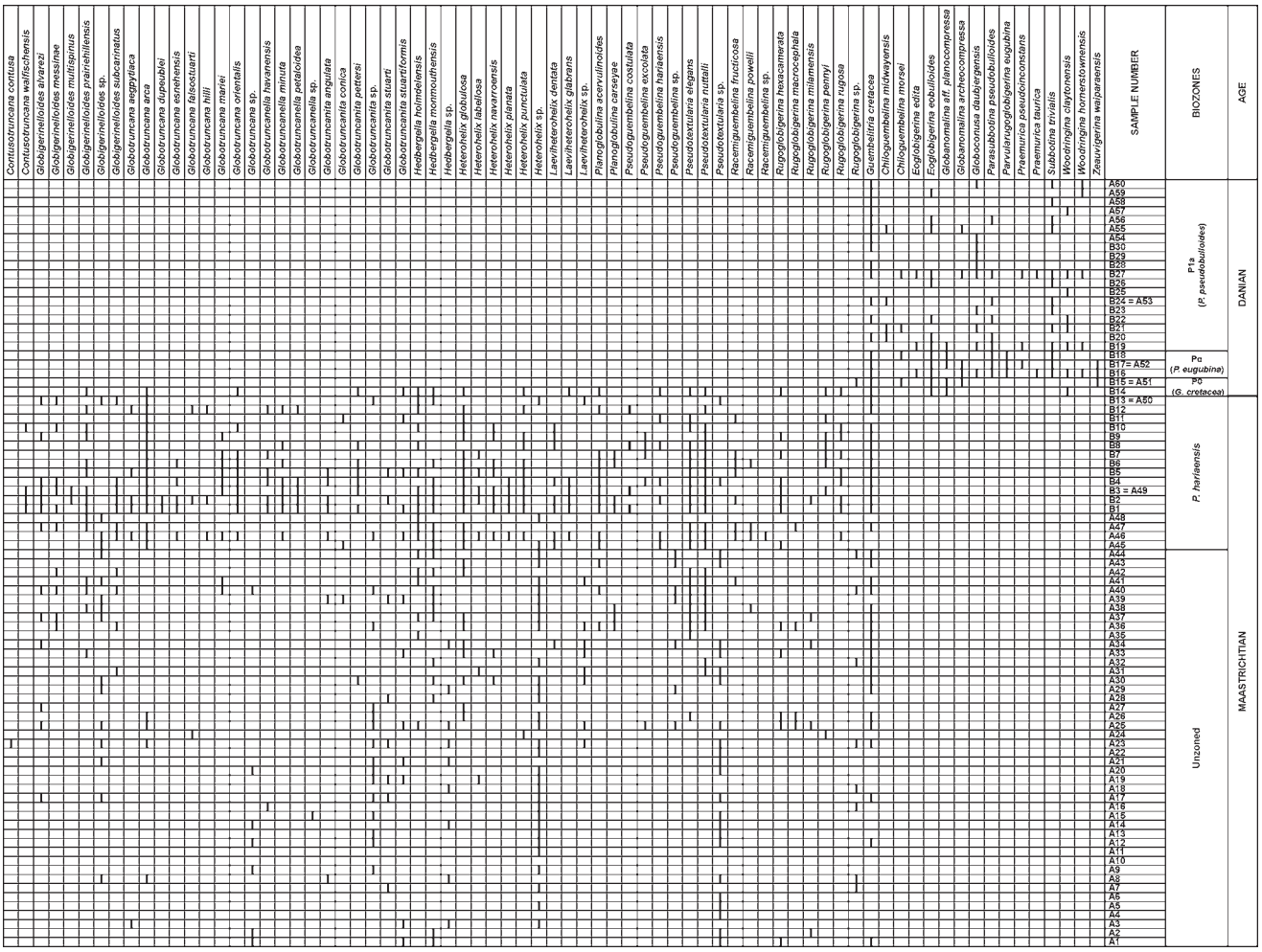

Biostratigraphy

The biostratigraphy of the measured section is based on planktonic foraminiferal datum events (Table 1). Fourteen genera and 47 species indicative of the Maastrichtian and 10 genera and 15 species indicative of the Danian were identified. Due to the rareness and absence of coiled index taxa in the uppermost Maastrichtian, we used the Tethyan biozonation of Robaszynski and Caron (1995) and Robaszynski (1998) that is based on biserial (Heterohelicidae) families. This standard heterohelicid biozonation, although based on Mediterranean sections, is globally applicable and has been used by many authors in various K/Pg boundary localities where globotruncanids are absent or rare (e.g., Li and Keller 1998; Obaidalla 2005; Georgescu and Abramovich 2008; Huber et al. 2008). For the lowermost Paleogene, we used the standard zonal scheme of Olsson et al. (1999) and Berggren and Pearson (2005).

We recognize four upper Maastrichtian to lower Danian biozones: the *Pseudoguembelina hariaensis* Zone, Zone P0 (*Guembelitria cretacea*), Zone Pα (*Parvularugoglobigerina eugubina*), and Zone P1a (*Parasubbotina pseudobulloides*) from older to younger (Table 1). In the lowermost part of the section (samples A1–A44), below the *P. hariaensis* Zone, carbonates and marls representing a shallow-water paleoenvironment have very few planktonic foraminifera to assign biozones. However, some upper Maastrichtian index taxa exist in this unzoned interval, such as *Planoglobulina acervulinoides* (lowest occurrence in sample A36) and *Racemiguembelina fructicosa* (lowest occurrence in sample A41), whose lowest occurrences in the section seem to be facies controlled (Table 1). In addition, there is an ~ 2-m-thick covered interval in the outcrop below sample A40 where we could not sample (Fig. 2). This may have also caused us to miss the global first appearance datum of *R. fructicosa* (Fig. 4).

***Pseudoguembelina hariaensis* Partial-Range Zone.**—The *P. hariaensis* Partial-range Zone (Robaszynski and Caron 1995) is the interval from the first appearance datum (FAD) of the nominate species to the extinction horizon of the Cretaceous planktonic foraminifera at the K/Pg boundary, such as *Globotruncana aegyptiaca*, *Globotruncana arca*, *Globotruncanita stuarti*, *Globotruncanita stuartiformis*, *Globigerinelloides multispinus*, *Globigerinelloides subcarinatus*, *Racemiguembelina fructicosa*, *Rugoglobigerina hexacamerata*, *Rugoglobigerina macrocephala*, *Rugoglobigerina rugosa*, and *Pseudotextularia elegans*. The *P. hariaensis* Zone in the

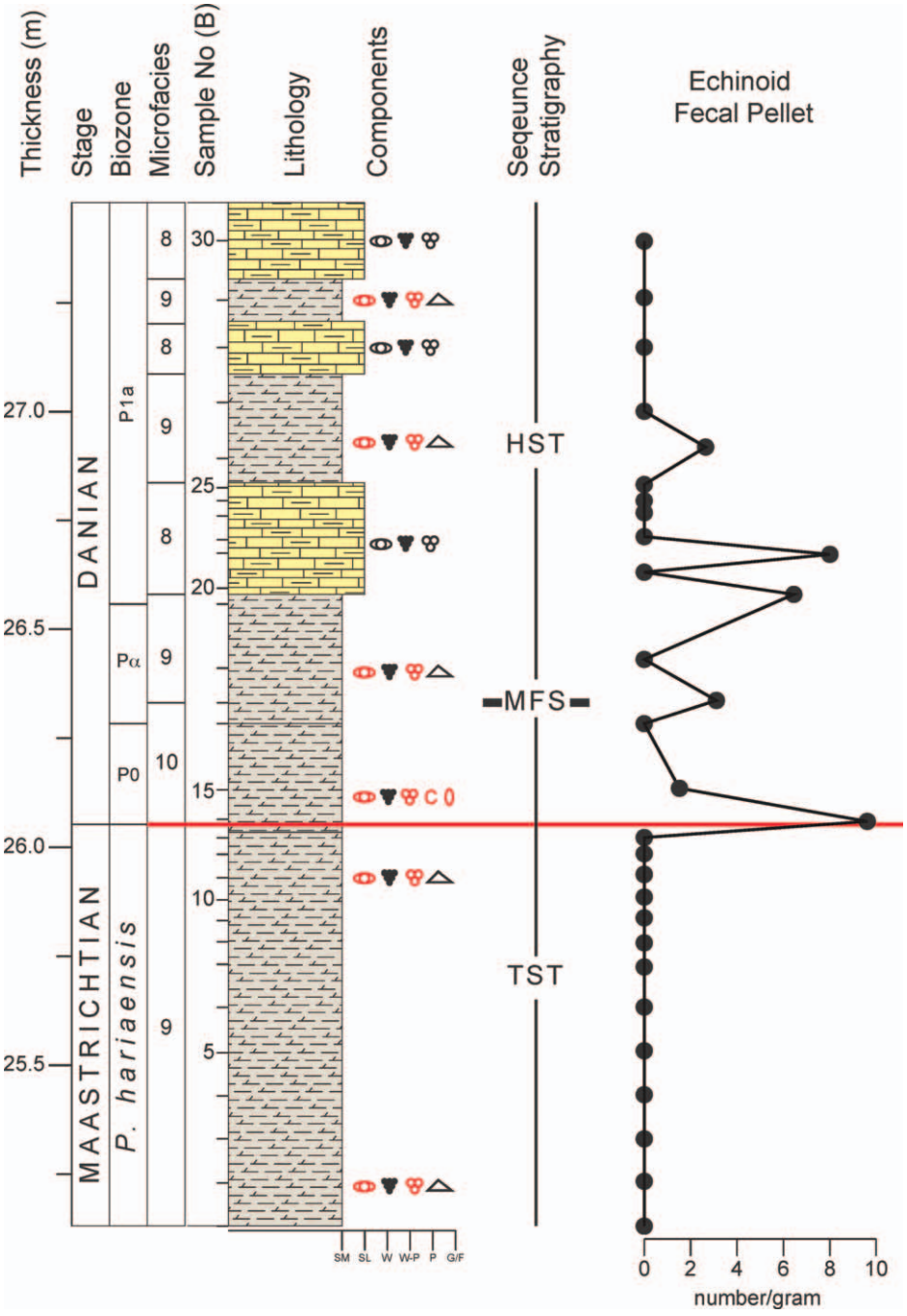

FIG. 3.—Lithostratigraphy, planktonic foraminiferal biozones, microfacies types, sequence stratigraphical interpretation, and counts of echinoid fecal pellets of the closely sampled section across the K/Pg boundary (Samples B1–B30). The following samples represent the same stratigraphic horizon: A49 = B3, A50 = B13, A51 = B15, A52 = B17, A53 = B24. Refer to the legend in Figure 2. The most abundant biogenic and abiogenic components are shown in red. HST, highstand systems tract; TST, transgressive systems tract; TS, transgressive surface; MFS, maximum flooding surface.

measured section is ~ 5 m thick (samples A45–A50/B13) and lies within the silty marls rich in quartz and iron-oxide (Table 1, Fig. 4).

Zone P0 (*Guembelitria cretacea* Partial-Range Zone).—This zone is the lowermost Danian zone and is defined by the partial range of the nominate taxon between the LAD of Cretaceous genera like *Globotruncana*, *Globotruncanita*, *Contusotruncana*, *Globotruncanella*, *Rugoglobigerina*, *Racemiguembelina*, *Planoglobulina*, and the FAD of *Parvularugoglobigerina eugubina* (Olsson et al. 1999; Berggren and Pearson 2005; Wade et al. 2011). It is represented in the section from samples B14 to B15. Early-evolved Danian forms observed in this interval are *Eoglobigerina eobulloides*, *Globanomalina archeocompressa*, *Zeauvigerina waiparaensis*, and *Globanomalina* aff. *planocompressa* (Table 1, Fig. 5). *Guembelitria cretacea* is also abundant. In this zone except these forms, which typically appear in P0, we also identified biserial forms like *Woodringina claytonensis* and *Chiloguembelina morsei*. According to the Atlas of Paleocene Planktonic Foraminifera (Olsson et al. 1999) biserial species only evolve in Zone Pα, but several other authors observed them in Zone P0 (Keller 1988; Koutsoukos 1996; Luciani 2002).

We found *G.* aff. *planocompressa* in Zone P0 starting from the first Danian sample. It is a low trochospiral form with 3–3.5 chambers resembling the species first described by Luterbacher and Premoli-Silva (1964) as *Globigerina minutula* in the Gubbio section, Italy together with "*Globigerina*" *eugubina*. Later, *Globigerina minutula* was used as a zonal

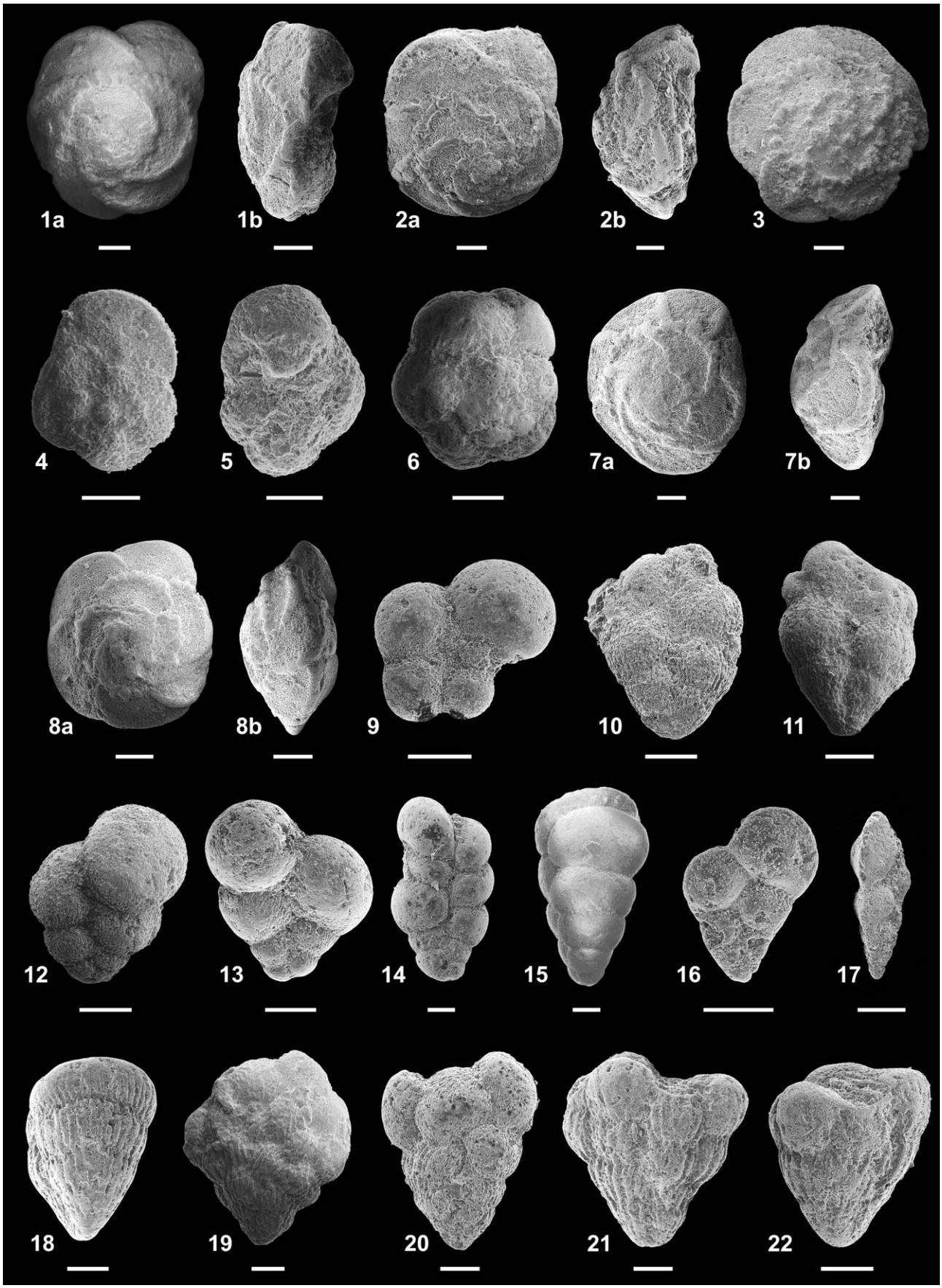
1a
1b
2a
2b
3
4
5
6
7a
7b
8a
8b
9
10
11
12
13
14
15
16
17
18
19
20
21
22

species for the early Danian after the *G. cretacea* Zone and before "*Globigerina*" *fringa* and "*Globigerina*" *eugubina* Zones (Smit 1982). After that, the species has been described as an early Danian form by many authors with various different names (Keller 1988; Huber 1991; Liu and Olsson 1992; Luciani 1997; Obaidalla 2005; Arenillas et al. 2006). *Globigerina minutula* was not included in the Atlas of Paleocene Planktonic Foraminifera (Olsson et al. 1999) because the type specimen was completely recrystallized and the wall structure is unknown. The species we described in the Haymana Basin from P0 to lower P1a mostly resembles *Globanomalina planocompressa* with its low, umbilical–extraumbilical aperture bordered by a narrow lip, axial compression, and smooth wall (Fig. 5.1a, 5.1b). Since *G. planocompressa* has five chambers in the last whorl, this form should be an earlier morphological variant of the species and shall be named as *G.* aff. *planocompressa*.

Besides the first Paleocene forms, some Cretaceous forms are also observed in the first Danian sample (B14) such as *Globotruncana arca, Globotruncana orientalis, Globotruncanita pettersi, Globotruncanita stuartiformis, Rugoglobigerina hexacamerata, Rugoglobigerina pennyi, Rugoglobigerina rugosa, Globigerinelloides prairiehillensis, Heterohelix globulosa, Heterohelix punctulata, Pseudotextularia elegans, Pseudotextularia nuttalli, Planoglobulina acervulinoides, Pseudoguembelina hariaensis, Laeviheterohelix glabrans, H. holmdelensis, H. monmouthensis*, and *G. cretacea*. All these Cretaceous forms occur only within the first 5 cm of the Danian strata, their relative abundance is lower than the occurrences in the Maastrichtian, and they do not exist further in the section. Therefore, we consider them as reworked species.

Among the Cretaceous fauna that we observed in the first Danian sample, only *G. cretacea* continues up in the section into Zone P1a (Table 1). *Guembelitria cretacea* is considered as a survivor, and all microperforate Cenozoic species are phylogenetically related to *G. cretacea* based on wall structure and other morphologic characteristic (Olsson et al. 1999).

Zone Pα (*Parvularugoglobigerina eugubina* Taxon-Range Zone).—The *Parvularugoglobigerina eugubina* Total Range Zone, also called Zone Pα, is the interval characterized by the total range of the nominate taxon (Berggren et al. 1995; Olsson et al. 1999; Wade et al. 2011). Zone Pα in the section occurs between samples B16–B18. It includes the following species: *G. cretacea*, *G.* aff. *planocompressa*, *G. archeocompressa*, *Globoconusa daubjergensis*, *Woodringina hornerstownensis*, *W. claytonensis*, *E. eobulloides*, *Eoglobigerina edita*, *Subbotina trivialis*, *C. morsei*, *Z. waiparaensis*, *P. eugubina*, *Praemurica taurica*, *Praemurica pseudoinconstans*, and *P. pseudobulloides* (Table 1, Fig. 5).

Zone P1a (*Parasubbotina pseudobulloides* Partial-Range Subzone).—Zone P1a is the *Parvularugoglobigerina eugubina–Subbotina triloculinoides* Interval Subzone. It is defined as the biostratigraphic interval between the LAD of *P. eugubina* and the FAD of *S. triloculinoides* (Olsson et al. 1999; Berggren and Pearson 2005). The zone starts in sample B19, above the LAD of *P. eugubina* and continues to the top of the measured section (Table 1, Fig. 5). Important forms observed in this zone are: *G. cretacea*, *G. daubjergensis*, *W. hornerstownensis*, *W. claytonensis*, *E. eobulloides*, *E. edita*, *S. trivialis*, and *G. archeocompressa*.

Microfacies Analysis

The objective of the microfacies analysis is to integrate sedimentological and paleontological results to evaluate the depositional history of the section spanning the K/Pg boundary. We determined 10 microfacies (MF) types corresponding to inner-ramp to basin environments (Fig. 6) using mineralogical components, macrofossil and microfossil assemblages (Fig. 7), and texture of the samples observed in thin sections and outcrop. All microfacies types were deposited on an unrimmed shelf with no reef-derived components.

MF1: Bioclastic Packstone with Large Benthic Foraminifera and Calcareous Red Algae.—Yellowish colored bioclastic packstone at the lowermost part of the section (samples A1–A9 and A12–A14) is characterized by abundant macrofossil and microfossils in a micritic matrix (Figs. 2, 8A, B). Large hyaline benthic foraminifera such as *Orbitoides*, *Lepidorbitoides*, *Siderolites*, *Sulcoperculina*, and *Hellenocyclina* are highly diversified. Agglutinated uncoiled benthic foraminifera and corallinacean and solenoporacean calcareous red algae are abundant. Mollusk fragments (pelecypoda, gastropoda, and cephalopoda), echinoderm fragments and spines, bryozoans, and calcareous green algae are also present. Planktonic foraminifera are present but rare. The size of the allochems is coarse and the percentage of the micritic matrix shows variability within the microfacies. In some samples sparitic calcite is also seen in low amounts.

MF1 corresponds to an inner-ramp environment, which is above the fair-weather wave base (FWWB), and restricted to open marine conditions (Fig. 6). Large rotaliinid benthic foraminifera are rock forming in restricted and open marine environments in the platform interiors and inner ramps (Flügel 2004). Furthermore, calcareous red algae occur only in the photic zone and in the platform margins and inner-ramp to mid-ramp settings (Flügel 2004). Bryozoans, mollusks, and echinoderms are also seen in inner-ramp and mid-ramp settings and platform-interior to slope environments.

This microfacies is equivalent to the standard microfacies (SMF) 18-FOR (bioclastic grainstones and packstones with abundant benthic foraminifera or calcareous algae; "FOR" denotes abundance of foraminifera) and ramp microfacies (RMF) 13 (packstone with abundant larger foraminifera) of Flügel (2004). It is also equivalent to facies zone (FZ) 7 (platform interior, open marine) of Wilson (1975).

←

FIG. 4.—Scanning-electron-microscope images of Maastrichtian planktonic foraminifera species. Scale bar represents 100 μm. **1)** *Globotruncana arca* CUSHMAN, sample no. B1, *P. hariaensis* Zone, **a)** spiral view, **b)** side view. **2)** *Globotruncana orientalis* EL NAGGAR, sample no. B5, *P. hariaensis* Zone, **a)** spiral view, **b)** side view. **3)** *Globotruncana dupeublei* CARON et al., sample no. B1, *P. hariaensis* Zone, spiral view. **4)** *Globotruncana aegyptiaca* NAKKADY, sample no. B2, *P. hariaensis* Zone, spiral view. **5)** *Globotruncana aegyptiaca* NAKKADY, sample no. B1, *P. hariaensis* Zone, umbilical view. **6)** *Rugoglobigerina pennyi* BRONNIMANN, sample no. B3, *P. hariaensis* Zone, spiral view. **7)** *Globotruncana stuarti* de LAPPARENT, sample no. B5, *P. hariaensis* Zone, **a)** spiral view, **b)** side view. **8)** *Globotruncanita stuartiformis* DALBIEZ, sample no. B5, *P. hariaensis* Zone, **a)** spiral view, **b)** side view. **9)** *Globigerinelloides subcarinatus* BRONNIMANN, sample no. A46, *P. hariaensis* Zone, spiral view. **10)** *Pseudoguembelina hariaensis* NEDERBRAGT, sample no. B2, *P. hariaensis* Zone, side view. **11)** *Pseudoguembelina hariaensis* NEDERBRAGT, sample no. A46, *P. hariaensis* Zone, side view. **12)** *Heterohelix globulosa* EHRENBERG, sample no. B2, *P. hariaensis* Zone, side view. **13)** *Heterohelix globulosa* EHRENBERG, sample no. A46, *P. hariaensis* Zone, side view. **14)** *Pseudotextularia nuttalli* VOORWIJK, sample no. B5, *P. hariaensis* Zone, side view. **15)** *Pseudotextularia nuttalli* VOORWIJK, sample no. B5, *P. hariaensis* Zone, edge view. **16)** *Laeviheterohelix glabrans* CUSHMAN, sample no. A46, *P. hariaensis* Zone, side view. **17)** *Laeviheterohelix glabrans* CUSHMAN, B14, *P. hariaensis* Zone, edge view. **18)** *Pseudotextularia elegans* RZEHAK, sample no. B3, *P. hariaensis* Zone, edge view. **19.** *Planoglobulina acervulinoides* EGGER, sample no. B1, *P. hariaensis* Zone, side view. **20)** *Planoglobulina carseyae* PLUMMER, sample no. B2, *P. hariaensis* Zone, side view. **21.**) *Racemiguembelina fructicosa* EGGER, sample no. A46, *P. hariaensis* Zone, side view. **22)** *Racemiguembelina powelli* SMITH and PESSAGNO, sample no. A46, *P. hariaensis* Zone, side view.

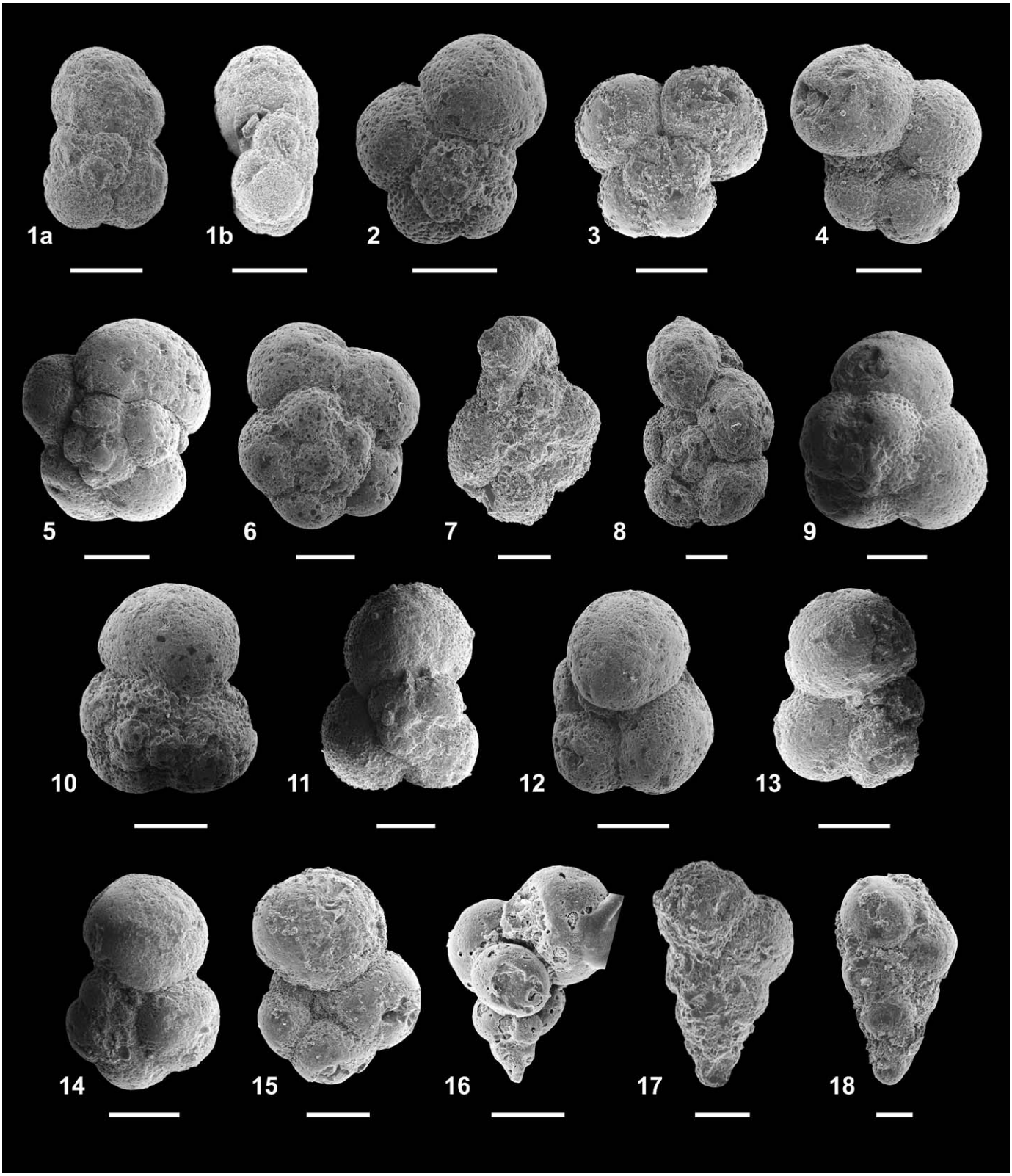
1a
1b
2
3
4
5
6
7
8
9
10
11
12
13
14
15
16
17
18

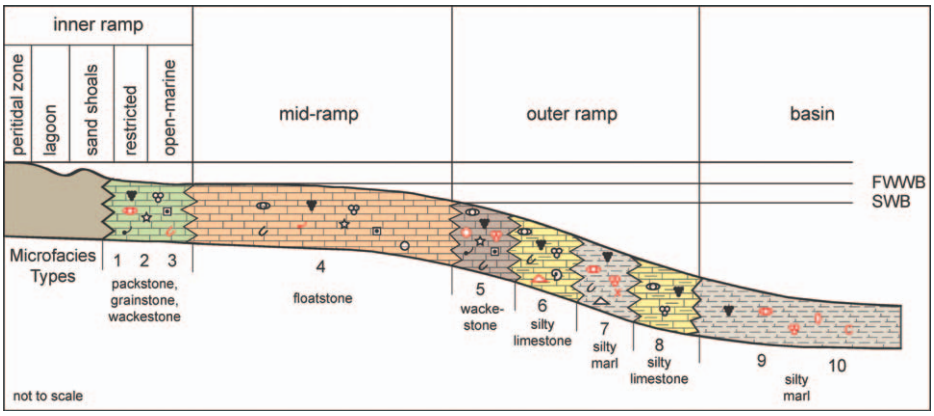

FIG. 6.—Model showing the paleoenvironment and lateral relationship of the microfacies types. Modified after model of ramp microfacies types of Flügel (2004). Refer to the legend in Figure 2. FWWB, fair-weather wave base; SWB, storm wave base.

MF2: Grainstone with Large Benthic Foraminifera and Calcareous Red Algae.—MF2 is characterized by abundant large benthic foraminifera and calcareous red algae in sparitic cement and identified in samples A10 and A11 (Figs. 2, 8C, D). The most common large benthic foraminifera in MF2 are *Orbitoides*, *Lepidorbitoides*, *Omphalocyclus*, *Siderolites*, *Sulcoperculina*, and *Hellenocyclina*. Bryozoans and agglutinated benthic foraminifera are common and mollusk and echinoderm fragments are also present.

MF2 is similar to MF1 except the sparitic calcite content of the former. It represents a high-energy environment above the FWWB (Fig. 6). It can be considered equivalent to the SMF18 of Flügel (2004), which is composed of bioclastic grainstones and packstones with abundant benthic foraminifera or calcareous algae. It is also equivalent to FZ7 of Wilson (1975), which corresponds to an inner-ramp environment with restricted or open marine conditions.

MF3: Bioclastic Wackestone–Packstone with Benthic Foraminifera and Calcareous Red Algae.—This microfacies type occur in the lower parts of the measured section in samples A15, A16, A18, and A23 (Fig. 2). It is similar to MF1 and MF2 in terms of faunal content. However, the amount of micrite and the size and the abundance of the allochems are lower in this microfacies (Fig. 8E, F). Hyaline benthic foraminifera and calcareous red algae are abundant. Agglutinated benthic foraminifera, echinoderm spines, bryozoans, and mollusk fragments are quite common, and calcareous green algae and some calcispheres are also observed. Planktonic foraminifera are rare. Considering its texture and fossil content, MF3 belongs to an environment above the FWWB and corresponds to SMF18-FOR and RMF13 of Flügel (2004) like MF1 and MF2 (Fig. 6).

MF4: Bivalved Floatstone.—MF4 is in samples A17 and A19–A22 and composed of large mollusks, especially bivalve fragments (Fig. 8G, H). The shell fragments exceed 2 mm in size and constitute almost 50% of the rock embedded in a micritic matrix. In between the bivalve fragments there are planktonic and benthic foraminifera and micritic mud containing calcispheres. The size of the foraminifera and other bioclasts within the shell pieces is very small. Besides bivalves, foraminifera and calcispheres, echinoderms, bryozoans, calcareous red and green algae are quite common, whereas large hyaline benthic foraminifera are rare in MF4.

MF4 is very similar to the SMF12-Bs (Bs stands for bivalves) defined by Flügel (2004). The SMF12-Bs was defined as densely packed floatstones characterized by accumulations of one-type-of-shell concentration. Bivalve shell beds can be found in a wide range of environments from platform-interior settings and inner-ramp to deep-marine settings (Flügel 2004). Because the shell concentrations are seen in a micritic matrix abundant in pelagic organisms, we concluded that this facies was deposited in a mid-ramp environment between FWWB and storm wave base (SWB) (Fig. 6).

MF5: Wackestone with Planktonic Organisms.—MF5 is in samples A24–A26 and characterized by its very fine micritic matrix containing common planktonic foraminifera and calcispheres. Besides the planktonic organisms, it also contains hyaline and agglutinated benthic foraminifera, calcareous red algae, mollusk fragments, bryozoans, and echinoderms (Fig. 9A, B).

In this facies, we identified common planktonic foraminifera in association with algae and benthic foraminifera indicating a deepening in the section. Although the number of planktonic foraminifera increases in this facies relative to the MF1–4, large benthic foraminifera (e.g.,

←

FIG. 5.—Scanning-electron-microscope images of Danian planktonic foraminifera species. Scale bar represents 100 μm for 1–15 and 50 μm for 16–18. **1)** *Globanomalina* aff. *planocompressa* SHUTSKAYA, sample no. B14, Zone P0, **a)** spiral view, **b)** side view. **2)** *Eoglobigerina eobulloides* MOROZOVA, sample no. B27, Zone P1a, spiral view. **3)** *Eoglobigerina eobulloides* MOROZOVA, sample no. B19, Zone P1a, spiral view. **4)** *Eoglobigerina eobulloides* MOROZOVA, sample no. B19, Zone P1a, umblical view. **5)** *Eoglobigerina edita* SUBBOTINA, sample no. B27, spiral view, Zone P1a, spiral view. **6)** *Eoglobigerina edita* SUBBOTINA, sample no. B27, spiral view, Zone P1a, spiral view. **7)** *Parvularugoglobigerina eugubina* LUTERBACHER and PREMOLI-SILVA, sample no. B16, Zone P1a, spiral view. **8)** *Praemurica taurica* MOROZOVA, sample no. B27, Zone P1a, spiral view. **9)** *Subbotina trivialis* SUBBOTINA, sample no. B27, Zone P1a, spiral view. **10)** *Subbotina trivialis* SUBBOTINA, sample no. B27, Zone P1a, spiral view. **11)** *Subbotina trivialis* SUBBOTINA, sample no. B17, Zone Pα, spiral view. **12**) *Subbotina trivialis* SUBBOTINA, sample no. B27, Zone P1a, umbilical view. **13)** *Subbotina trivialis* SUBBOTINA, sample no. B19, Zone P1a, umblical view **14)** *Parasubbotina pseudobulloides* PLUMMER, sample no. B16, Zone Pα, spiral view. **15)** *Parasubbotina pseudobulloides* PLUMMER, sample no. B19, Zone P1a, umbilical view. **16.**) *Guembelitria cretacea* CUSHMAN, sample no. A60, Zone P1a, side view. **17)** *Woodringina claytonensis* LOEBLICH and TAPPAN, sample no. B14, Zone P0, side view. **18)** *Woodringina claytonensis* LOEBLICH and TAPPAN, sample no. B16, Zone Pα, side view.

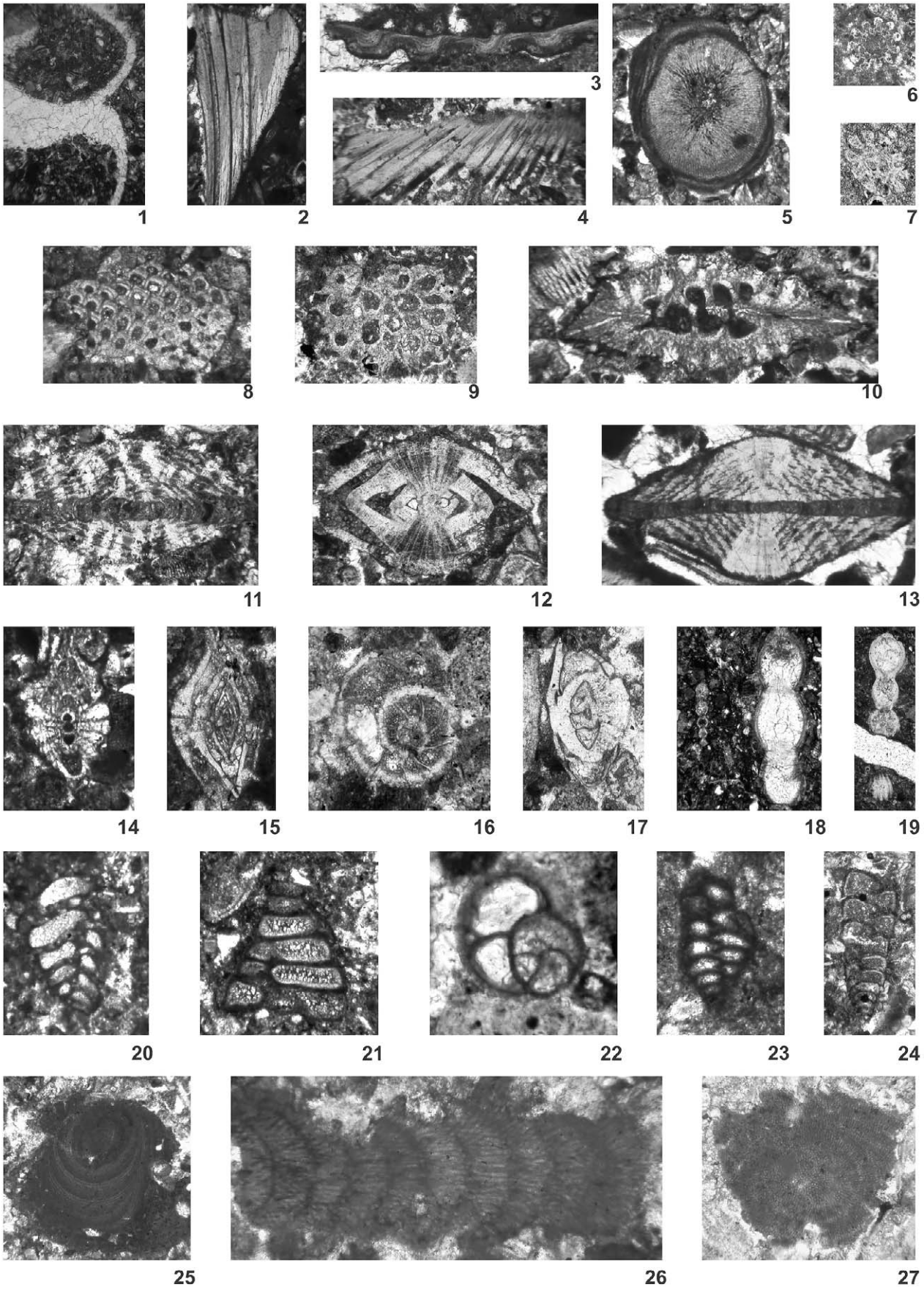
1
2
3
4
5
6
7
8
9
10
11
12
13
14
15
16
17
18
19
20
21
22
23
24
25
26
27

Helenocyclina) are still common. Middle-neritic to outer-neritic hyaline benthic foraminifera (e.g., *Nodosaria*) also exist in MF5. *Nodosaria* in association with planktonic foraminifers indicate a deeper shelf environment (Geel 2000). Hence, we concluded that MF5 was deposited below SWB in a mid-ramp to outer-ramp setting (Fig. 6).

MF6: Quartz-Rich Silty Limestone with Benthic and Planktonic Foraminifera and Calcareous Red Algae.—This facies was described as dark gray, silty limestone in the field and includes samples A27–A30, A34–A35, and A38–A39 (Fig. 2). It is quartz-rich and silty; however, the calcium carbonate matrix is the dominant constituent. The facies is fossiliferous and contains agglutinated benthic foraminifera, hyaline smaller benthic foraminifera, planktonic foraminifera, bryozoans, mollusk fragments, echinoderm spines, and calcareous red algae (Fig. 9C, D). Benthic foraminifera and calcareous red algae are especially dominant. The number of middle-neritic to outer-neritic smaller benthic foraminifera like *Nodosaria* increases in the facies relative to their abundance in the older levels in the measured section.

MF6 shows characteristics of proximal outer-ramp settings (Fig. 6). The model established by El Gadi and Brookfield (1999) and the RMF model proposed by Flügel (2004) place the marly facies in the outer-ramp settings, below SWB. In addition, Heldt et al. (2008) has defined the silty limestone facies with planktonic and small benthic foraminifera and shell fragments in proximal outer ramp settings.

MF7: Iron-Rich Silty Marl with Planktonic and Benthic Foraminifera.—This facies was described as dark gray marl in the field. It is one of the most common MF types in the studied section and spans the Upper Cretaceous sediments towards to the K/Pg boundary beds in samples A30–A34, A36–A38, and A40–A48 (Figs. 2, 9E, F). Iron and clay minerals are very rich, and most shells are filled with iron-oxide minerals. Quartz and feldspar grains are also common in this facies. The sizes of quartz grains are usually larger than those of quartz grains seen in MF6. Although there are some red algae and other bioclasts, the main fossils in MF7 are smaller benthic and planktonic foraminifera. This marly facies was deposited in low-energy settings below SWB. The dominance of deeper-water benthic and planktonic foraminifera indicate a proximal outer-ramp setting (Fig. 6).

MF8: Silty Limestone with Planktonic and Benthic Foraminifera.—This facies found in the Danian has been observed as a yellowish-brownish limestone in the field and is represented by samples B20–B25, B28, B30, A56, A58, and A60 (Figs. 2, 3). This silty limestone is rich in clay minerals and contains planktonic and small hyaline and agglutinated benthic foraminifera (Fig. 9G–H). The early Paleocene planktonic foraminifera are small and commonly filled with iron minerals.

Based on its textural and compositional properties, MF8 indicates deposition below SWB, in low-energy settings. It resembles MF6, but the greater abundance of planktonic foraminifera than benthic foraminifera, as well as the absence of calcareous algae, indicates proximity to the basin. It should also be noted that the increase in the number of planktonic foraminifera in MF8 upsection might reflect the recovery of Danian planktonic foraminifera after the K/Pg mass extinction and might not be solely controlled by depositional settings. The number of planktonic foraminifera is slightly less in this facies than in MF9 and MF10, indicating that MF8 represents a shallower paleoenvironment. We consider MF8 as an outer-ramp facies (Fig. 6).

MF9: Silty Marl with Planktonic and Benthic Foraminifera.—This facies was described as greenish gray marl in outcrop and is found in the lowermost Danian. It is represented by samples B1–B13, B16–B19, B26, B27, B29, A55, A57, and A59 (Figs. 2, 3). MF9 has a marly character consisting of silt-size siliciclastic particles and micrite, rich in planktonic foraminifera and agglutinated and smaller hyaline benthic foraminifera (Fig. 10A, B).

MF9 has characteristics similar to MF7 in terms of texture and composition. However, the main difference between MF9 and MF7 is the iron-oxide rich composition of the latter and the abundance of planktonic foraminifera in MF9, indicating a paleoenvironment below SWB (Fig. 6). Furthermore, MF9 has a greenish color due to the enrichment of clay minerals.

MF10: Silty Marl with Clay Minerals and Fecal Pellets.—MF10 corresponds to lowermost Danian beds in samples B14, B15/A51, and B17/A52 (Figs. 2, 3). It is a marly unit that has both micritic matrix and silt-size siliciclastic material and is characterized by benthic and planktonic foraminifera. Large agglutinated noncoiled benthic foraminifera are common. Hyaline deep-sea benthic foraminifera displaying various sizes are also present. Early Danian planktonic foraminifera in this microfacies are very small and often filled with iron-oxide minerals (Fig. 10C, D).

In MF10, quartz and feldspar grains and green clay minerals showing rounded to angular shapes are very abundant. There is a prominent increase in clay minerals, including glauconite, smectite, and chlorite (Fig. 10E, F) and echinoid fecal pellets (Fig. 10G, I). The echinoid fecal pellets in the section are ~ 1-mm-long, orange to brown ellipsoidal grains with smooth surface (Fig. 10G–I). They were assigned to Echinodermata, especially of Echinoidea by Voigt (1929) and previously described in the lowest Paleocene in Denmark and Sweden in large quantities (Brotzen 1948; their Pl. 2, Fig. 2). Quantitative analysis of echinoid fecal pellets in both sections A and B shows that the number of pellets per gram of sample increases from 0 to12 in the first sample of Danian (A51 and B14; Figs. 2, 3). Some samples in section B (B17, B19, B21, B23; in Pα and lower P1a) still contain some echinoid fecal pellets, but their number goes to zero upsection (Fig. 3). MF10 represents a basin environment below the SWB similar to MF9 but slightly deeper (Fig. 6).

Sequence Stratigraphy and Sea-Level Changes

The measured section consists of three main sedimentary packages. The bottom of the section is composed of carbonate rocks (first package), the middle section is composed of a thick marly succession (second package), and the top is composed of carbonate–marl alternation (third package).

The first package consisting of carbonate rocks covers the upper Maastrichtian interval from sample A1 to sample A30 (Fig. 2). The MF types observed in this package are: bioclastic packstone with large benthic foraminifera and calcareous red algae (MF1); grainstone with large benthic foraminifera and calcareous red algae (MF2); bioclastic wack-

←

FIG. 7.—Photomicrographs of the major fossil groups identified for microfacies analysis. **1)** Gastropoda shell (×6, sample no. A21). **2**–**4)** Pelecypoda shell (2. ×10, sample no. A1. 3. ×15, sample no. A11. 4. ×7, sample no. A4). **5**–**7)** Echinodermata spine (5. ×16, sample no A7. 6. ×40, sample no. A19. 7. ×50, sample no. A26). **8–10)** Bryozoan shell (8. ×25, sample no. A8. 9. ×12, sample no. A17. 10. ×20, sample no. A8). **11**, **13**–**14)** Hyaline large benthic foraminifera (11. ×20, sample no. A1. 13. ×15, sample no. A11. 14. ×25, sample no. A1). **12**, **15**–**19)** Hyaline smaller benthic foraminifera (12. ×18, sample no. A3. 15. ×33, sample no. A2. 16. ×52, sample no. A13. 17. ×26, sample no. A1. 18. ×12, sample no. A14. 19. ×10, sample no. A25). **20**–**24)** Agglutinated benthic foraminifera (20. ×20, sample no. A16. 21. ×35, sample no. A24. 22. ×84, sample no. A22. 23. ×38, sample no. A15. 24. ×18, sample no. A6). **25**–**27)** Calcareous red algae (25. ×13, sample no. A2. 26. ×45, sample no. A4. 27. ×30, sample no. A2).

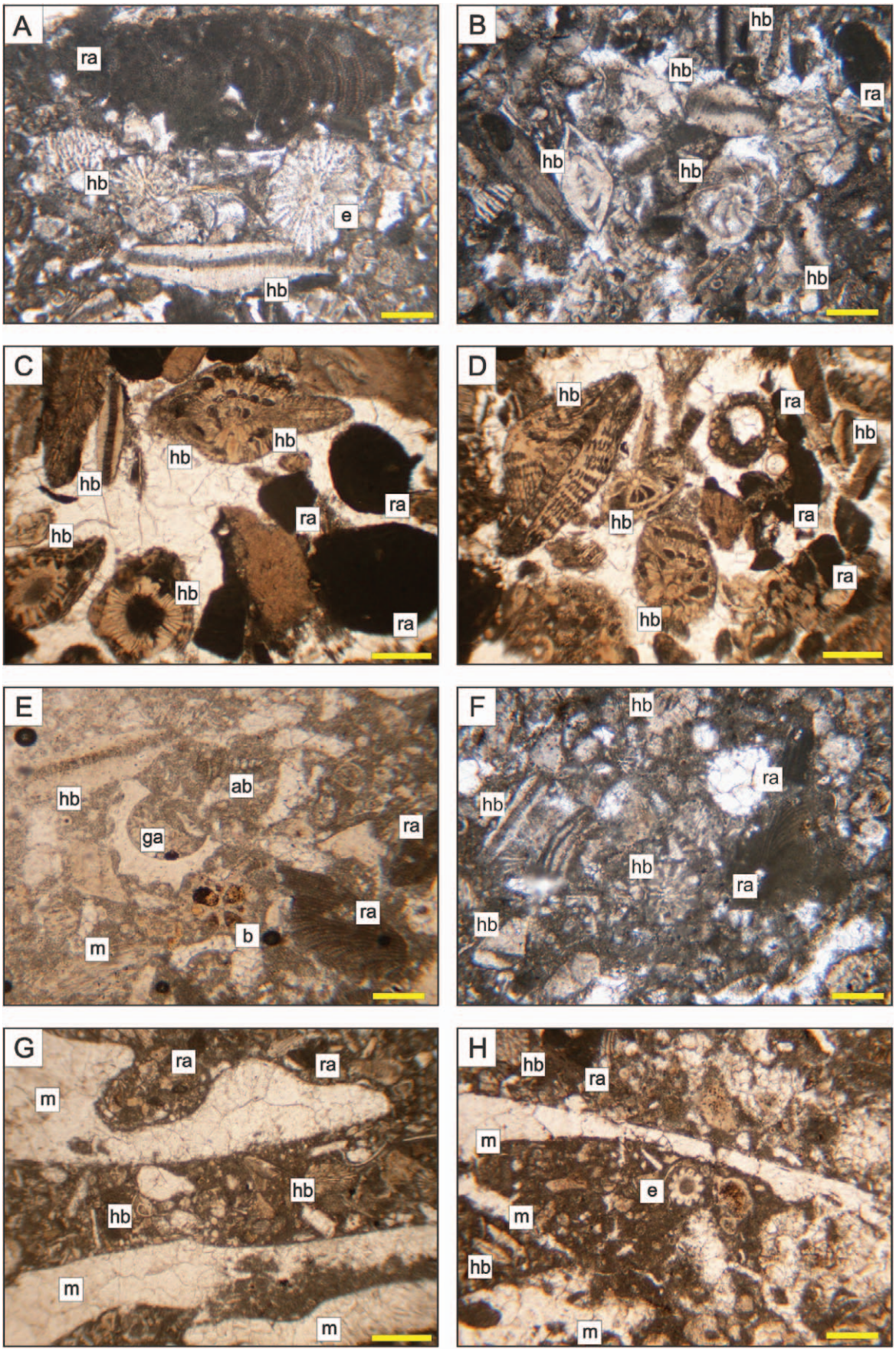
A
ra
hb
e
hb
B
hb
hb
ra
hb
hb
hb
C
hb
hb
hb
ra
ra
hb
hb
ra
D
hb
ra
hb
hb
ra
ra
hb
E
hb
ab
ra
ga
ra
b
m
F
hb
ra
hb
hb
ra
hb
G
ra
ra
m
hb
hb
m
m
H
hb
ra
m
e
m
hb
m

estone–packstone with benthic foraminifera and calcareous red algae (MF3); bivalved floatstone (MF4); and wackestone with planktonic organisms (MF5). The second package is composed of silty limestones and silty marls and covers the upper Maastrichtian to basal Danian interval from the sample A31 to A52/B17 (Figs. 2, 3). In this marly package we observe quartz-rich silty limestone with benthic and planktonic foraminifera and calcareous red algae (MF6), iron-rich silty marl with planktonic and benthic foraminifera (MF7), silty marl with planktonic and benthic foraminifera (MF9), and silty marl with clay minerals and fecal pellets (MF10). The third package is composed of silty marl (MF9)–silty limestone (MF8) alternations in samples A53 and A60.

The basic approach for the sequence stratigraphic interpretation of the section lies in the fact that carbonate rocks prograde into the basin when accommodation decreases and there is not enough space for carbonate growth. Carbonate growth is limited by the creation of accommodation and the deposition of carbonates takes place from a platform or an upslope top to the basin as "highstand shedding" (Emery and Myers 1996). In the highstand systems tract (HST), when the carbonate production exceeds the rate of creation of accommodation space, carbonates are shed off the platform top to the slope and basin, which is called the "keep up" phase (Neumann and Macintyre 1985). The first carbonate package in the section, consisting of mainly packstones and grainstones, was deposited during a HST, and high-energy carbonates of inner-ramp to mid-ramp (MF1–MF4) correspond to the keep-up phase. The carbonate source, which prograded into the basin during a HST, is considered to be the reefal and algal limestones of the Çaldağ Formation in the Haymana Basin.

Above the first carbonate succession, containing packstones, grainstones, wackestones, and wackestone with planktonic organisms such as planktonic foraminifera and calcispheres (MF5) was deposited during a deepening in the basin and a transition from mid-ramp to outer ramp (Fig. 6). Therefore, a transgressive surface (TS) is between the samples A23 and A24. Above the TS there is a package of quartz-rich silty limestones (MF6, samples A26–A30) containing planktonic foraminifera, benthic foraminifera, and ammonites indicating deepening, and above this unit transgression continues into the silty marls.

Silty marls (second package) start in the measured section at sample A30. As more accommodation is created with a relative sea-level rise, progradation of carbonates ceases and the transgressive systems tract (TST) starts. Silty marls indicate a general transgressive pattern until sample A52/B17 corresponding to an outer-ramp to basin environment (MF7, MF9).

The MFS is placed between samples A52 and A53 in section A and at sample B17 in section B, where the change from the distal basin (MF10) to proximal basin occurs (MF9). Above the MFS, alternation of distal outer-ramp silty limestones (MF8) and proximal basin silty marls (MF9) are observed (third package; Fig. 6). Above sample A52/B17, at sample A53, carbonates reappear in the measured section, indicating a HST (Figs. 2, 3). Progradation of the carbonates in the early Danian indicates the latest part of a relative sea-level rise. The K/Pg boundary is just below the maximum flooding surface (MFS), in the uppermost part of the TST.

We developed a relative sea-level curve (Fig. 11) for the section using our microfacies model (Fig. 6). We took the depth of inner-ramp–mid-ramp boundary (FWWB) as between 10 and 15 m and mid-rap–outer-ramp boundary (SWB) as 30 m (Burchette and Wright 1992) and estimated the relative paleowater depth of each MF type accordingly. Although absolute paleowater depths we assigned to the MF types might not be accurate, their relative positions to each other give us an idea about how relative sea level changed across the K/Pg boundary. The estimates of paleowater depth for the Haymana Basin indicated that maximum water depth was reached in MF10, just above the K/Pg boundary (Fig. 11), placing the boundary itself in a TST.

In order to test the sea-level changes across the K/Pg boundary in a different geographic location and compare it with the Haymana Basin, we studied a section in the Campo Pit, New Jersey (Fig. 11). The Campo Pit section was deposited in a shallow siliciclastic shelf environment sensitive to minor sea-level changes and shows a very similar history for sea-level changes across the K/Pg boundary, where the boundary is placed in a later phase of a TST, below a MFS (Fig. 11). In the section, white-yellowish, medium- to coarse-grained sandstone of the Redbank Formation is unconformably overlain by the yellowish-brownish, medium- to coarse-grained sandstone of the Tinton Formation (Fig. 11). The uppermost Redbank Formation represents an upper-shoreface environment with planar laminations and abundant vertical and horizontal *Ophiomopha* burrows. The overlying Tinton Formation at the Campo Pit shows a slight fining-upward succession with increased mud content. The top of the Tinton Formation at Campo Pit is a reddish indurated unit, which is overlain by the K/Pg boundary event bed. The event bed consists of red and green mud with basal clay clasts containing impact spherules. At the base of the event bed, the lowest occurrence of *Senoniasphaera inornata*, a dinoflagellate marker species, indicates the earliest Danian (Miller et al. 2010). Above the event bed, there is clayey green glauconitic sand of the Hornerstown Formation. Authigenic green glauconite of the Hornerstown Formation indicates an offshore environment below storm wave base. A MFS is associated with the maximum percentage of glauconite. In the HST, above the MFS there is a gradual increase in quartz grains indicating a shallowing. For the paleowater depth curve of Campo Pit (Fig. 11), we took the upper-shoreface–middle-shoreface boundary (FWWB) as between 10 and 15 m, the middle-shoreface–lower-shoreface boundary as 20 m, and the lower-shoreface–offshore boundary (SWB) as 30 m (Browning et al. 2008).

DISCUSSION

Planktonic foraminifera biostratigraphy indicates that the K/Pg transition is biostratigraphically complete in the Haymana section. In spite of the poor to moderate preservation of the foraminifera, index species defining the upper Maastrichtian and lower Danian biozones were identified. The basal part of the measured section (samples A1–A44) cannot be constrained at the level of biozones, because of the rareness of the planktonic foraminifera due to the facies control.

The Haymana Basin records an abrupt and catastrophic mass extinction of planktonic foraminifera. At the boundary, all the large, ornate, keeled forms of the genera *Globotruncana*, *Globotruncanita*, *Globotruncanella*, *Rugoglobigerina*, *Racemiguembelina*, *Pseudotextularia*, and *Pseudoguembelina* disappear. Above the extinction level, minute and delicate first Danian forms of the genera *Eoglobigerina*, *Globanomalina*, *Globoconusa*, and *Woodringina* appear.

←

FIG. 8.—Photomicrographs of the microfacies types. **A)** Bioclastic packstone with large benthic foraminifera and calcareous red algae (MF1), sample no. A1. **B)** Bioclastic packstone with large benthic foraminifera and calcareous red algae (MF1), sample no. A2. **C)** Grainstone with large benthic foraminifera and calcareous red algae (MF2), sample no. A10. **D)** Grainstone with large benthic foraminifera and calcareous red algae (MF2), sample no. A10. **E)** Bioclastic wackestone–packstone with benthic foraminifera and calcareous red algae (MF3), sample no. A18. **F)** Bioclastic wackestone–packstone with benthic foraminifera and calcareous red algae (MF3), sample no. A23. **G)** Bivalved floatstone (MF4), sample no. A19. **H)** Bivalved floatstone (MF4), sample no. A19. hb, hyaline benthic foraminifera; ab, agglutinated benthic foraminifera; p, planktonic foraminifera; ra, calcareous red algae; ga, calcareous green algae; m, mollusk fragment; b, bryozoan; e, echinodermata spine. Scale bar is 0.25 mm for A, B, E, F, H and 0.50 mm for C, D, and G.

←

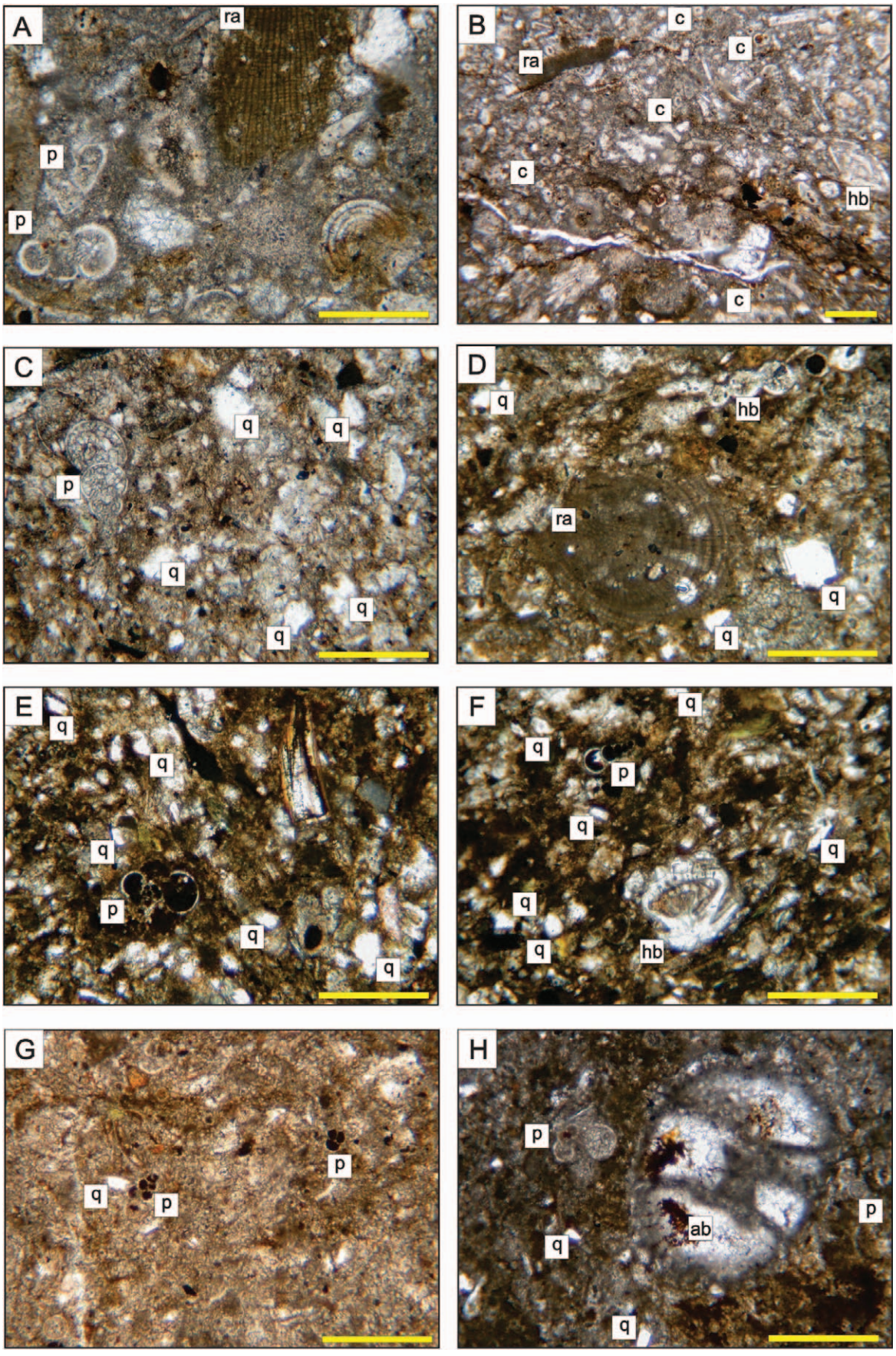
A
ra
p
p
B
c
c
ra
c
c
hb
c
C
q
q
p
q
q
q
D
q
hb
ra
q
q
E
q
q
q
p
q
q
F
q
q
p
q
q
q
q
hb
G
p
q
p
H
p
ab
q
p
q

In the first sample dated as Danian (B14), we encountered some Cretaceous taxa as well. Reworked specimens are difficult to identify unless they show differential preservation or a large age difference with the rest of the faunal assemblage. The Cretaceous species in our lower Danian sample do not show distinct characteristics that may enable us to decide whether they are survivor species or reworked species. However, except for *G. cretacea*, none of the species are seen up in the section above the first 5 cm of the Danian, and they are much lower in relative abundance relative to the Cretaceous samples. Therefore, we interpret that only *G. cretacea* survived the boundary. In fact, detailed taxonomic studies of the Paleogene Planktonic Foraminifera Working Group (Olsson et al. 1999) concluded that *G. cretacea* is one of the survivors of the K/Pg boundary mass extinction along with *H. holmdelensis* and *H. monmouthensis*.

Microfacies analysis indicated that deposition took place on an inner ramp (restricted and open marine conditions) with alternations of carbonates (packstones, grainstone, wackestones, and floatstones) to a basin with mixed siliciclastic–carbonate rocks (silty marls, silty limestones). The section is quite fossiliferous, having large hyaline benthic foraminifera, deeper-water hyaline, and agglutinated benthic foraminifera, mollusk shells, echinoderm spines, bryozoans, calcispheres, and corallinacean and solenoporacean red algae. The presence, absence, and abundances of these fossils were used in the determination of the environment of deposition in addition to textural properties of rocks.

For the sequence stratigraphic interpretation of the section, we considered overall geometry, depositional history, and geologic setting of the whole basin in addition to the microfacies analysis of the measured section. Our results indicate that the K/Pg boundary is recorded in the latest part of a TST, below a MFS. Enrichment of the authigenic clay minerals (Fig. 10E, F) just above the boundary (MF10) and below the MFS might also indicate a relative rise in sea level.

Although analysis of additional sections in the basin is necessary to have a more complete view on the environment of deposition and better constrain the sequence stratigraphy, the detailed microfacies analysis gives clues about the evolution of relative sea level. We constructed a relative sea-level curve for the Haymana Basin assigning paleowater depths to each MF type based on their relative positions to FWWB and SWB (Fig. 11). Our relative sea-level curve showed the TS and MFS clearly putting the K/Pg boundary in a late TST.

There is no consensus on global sea-level changes across the K/Pg boundary, likely due to the fact that the changes were subtle. The study of Vail et al. (1977) showed a major fall at the K/Pg boundary, whereas Haq et al. (1987) showed a 25 m sea-level rise from the K/Pg boundary into the Danian. Donovan et al. (1988) showed a major fall in the late Maastrichtian and a sea-level rise across the K/Pg boundary in Braggs section, Alabama. Olsson and Liu (1993) made important biostratigraphic revisions on the Braggs section (Donovan et al. 1988) and moved the boundary to a lower stratigraphic position. Accordingly, Olsson and Liu (1993) stated that sea level was at lowstand both before and after the boundary with a rise afterwards. Coarse-grained siliciclastic and limestone breccia deposits at the K/Pg boundary close to the impact site have been interpreted as pre-K/Pg sea-level lowstand deposits (Donovan et al. 1988; Keller and Stinnesbeck 1996; Keller 2007). However, this interpretation has been challenged by the fact that there are impact-generated tsunami deposits in these regions (e.g., Smit 1999) that have no relation to eustasy (e.g., Claeys et al. 2002).

European sections generally indicate a similar history for sea level across the K/Pg boundary in a number of locations: a SB below the boundary, with the K/Pg boundary placed within the overlying TST (Apellaniz et al. 1997; Pujalte 1998). Alegret et al. (2003) and Pardo et al. (1996) in Spain, and Pardo et al. (1999) in Kazakhstan indicated a sea-level rise across the K/Pg boundary. The global sea-level review of Keller and Stinnesbeck (1996) and the Tunisian record (Adatte et al. 2002) also showed a global sea-level rise across the K/Pg boundary into the Danian. We observe a very similar trend in the Haymana Basin, where the K/Pg boundary is placed in a late TST below a MFS.

Previous studies from New Jersey have provided important sea-level records from Cretaceous to Paleogene. Two major sea-level falls are recorded, one at the Campanian–Maastrichtian boundary (Miller et al. 2004) and the other at the base of the planktonic foraminiferal Zone P1b (Olsson et al. 2002). Benthic foraminiferal biofacies (Olsson et al. 2002) and backstripping results (Miller et al. 2005; Kominz et al. 2008) showed a minimal fall in sea level (< 25 m) associated with the K/Pg boundary, which is similar to the trend shown in the Haq curve (2014). However new data from the updip section, Campo Pit, show that the K/Pg boundary is within a sea-level rise in New Jersey (Fig. 11).

Detailed microfacies analysis of the Haymana Basin shows a sea-level history very similar not only to European and Tethyan sections (Keller and Stinnesbeck 1996; Pardo et al. 1996, 1999; Apellaniz et al. 1997; Pujalte 1998; Adatte et al. 2002) but also to the Campo Pit section, New Jersey, where the K/Pg boundary is in a TST (Fig. 11). This might indicate that the sea level in the Haymana Basin was controlled mainly by eustasy despite tectonic activity in the Central Anatolia. We acknowledge that reference frames for sea-level change are impacted by processes of regional tectonics and mantle dynamics (e.g., Moucha et al. 2008; Müller et al. 2008); however, these mechanisms largely affect the stratigraphic record on longer than million-year scales (e.g., Miller et al. 2005). Our observations of sea-level change in both the Haymana and Campo Pit sections are much shorter term, thus less likely impacted by these tectonic effects.

The increase in clay minerals like glauconite, smectite, and chlorite in the immediate aftermath of the K/Pg boundary in Zone P0 (sample A51/B15) might indicate an overall decrease in sedimentation rates, which is coupled with the drop in carbonate deposition mostly due to the mass extinction of carbonate-producing planktonic foraminifera and calcareous nannoplankton (Fig. 10E, F).

Another remarkable feature of Zone P0 is the prominent increase in echinoid fecal pellets (Fig. 10G–I). Our quantitative analysis indicates that echinoid fecal pellets appear in the first sample of the Danian just after the K/Pg boundary. They exist in the section up to lower P1a and then disappear again (Figs. 2, 3). Miller et al. (2010) reported an increase in echinoid fecal pellets in the lowermost Danian beds in several New Jersey paleoshelf downdip (i.e., deeper water) sections as well and suggested that this increase can be used as a stratigraphic horizon for the correlation of the K/Pg boundary. Our observation in the Haymana Basin supports the idea that the increase in the number of echinoid fecal pellets indicates an important environmental change after the K/Pg mass extinction and can be used as a marker for the K/Pg boundary in addition

←

FIG. 9.—Photomicrographs of the microfacies types. **A)** Wackestone with planktonic organisms (MF5), sample no. A25. **B)** Wackestone with planktonic organisms (MF5), sample no. A25. **C)** Quartz-rich silty limestone with benthic and planktonic foraminifera and calcareous red algae (MF6), sample no. A38. **D)** Quartz-rich silty limestone with benthic and planktonic foraminifera and calcareous red algae (MF6), sample no. A38. **E)** Iron-rich silty marl with planktonic and benthic foraminifera (MF7), sample no. A37. **F)** Iron-rich silty marl with planktonic and benthic foraminifera (MF7), sample no. A37. **G)** Silty limestone with planktonic and benthic foraminifera (MF8), sample no. A54. **H)** Silty limestone with planktonic and benthic foraminifera (MF8), sample no. A60. hb, hyaline benthic foraminifera; ab, agglutinated benthic foraminifera; p, planktonic foraminifera; ra, calcareous red algae; ga, calcareous green algae; m, mollusk fragment; b, bryozoan; e, echinodermata spine; c, calcispheres; q, quartz. Scale bar is 0.25 mm.

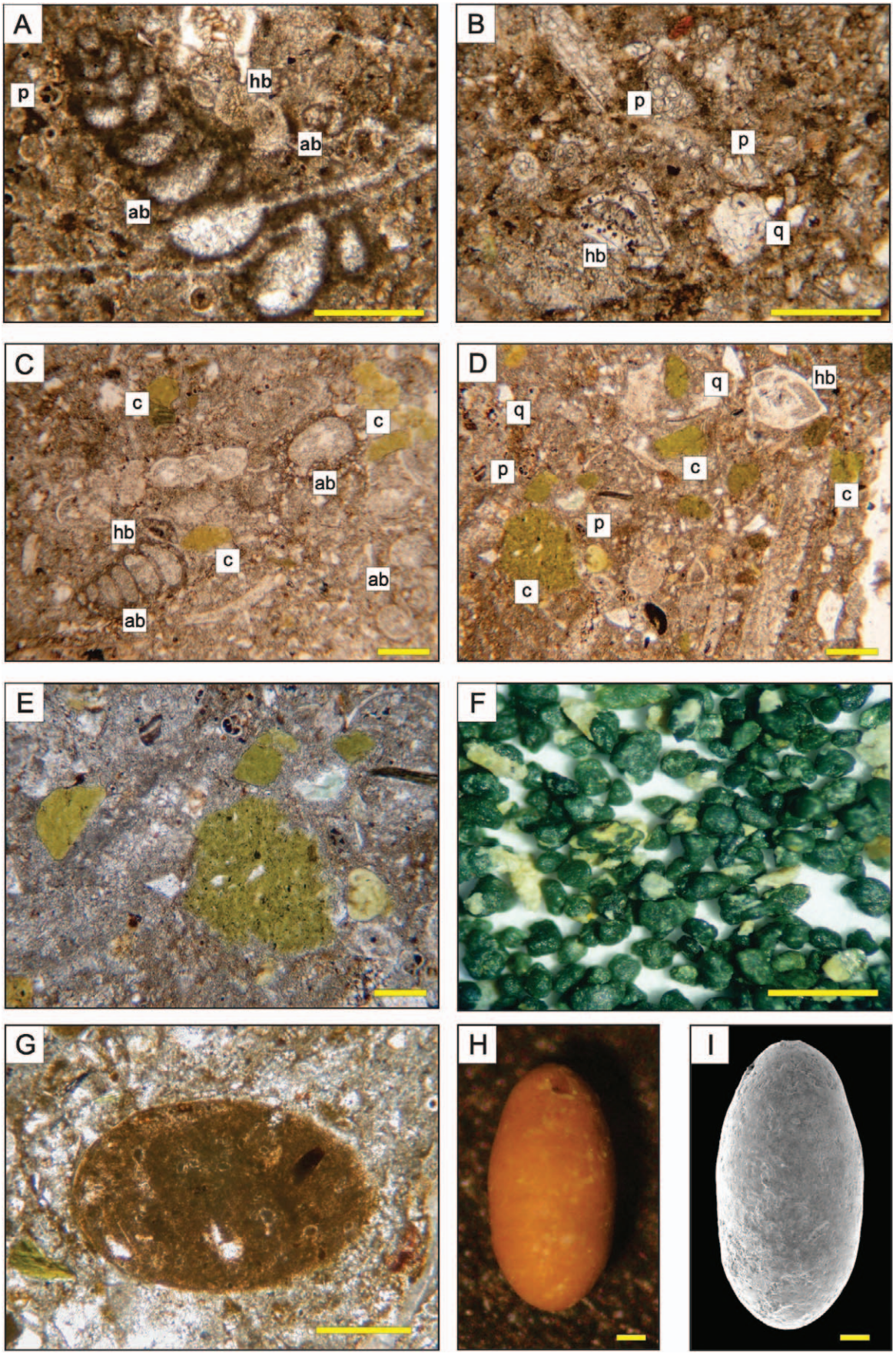
A
p
hb
ab
ab
B
p
p
q
hb
C
c
c
ab
hb
c
ab
ab
D
q
hb
q
p
c
c
p
c
E
F
G
H
I

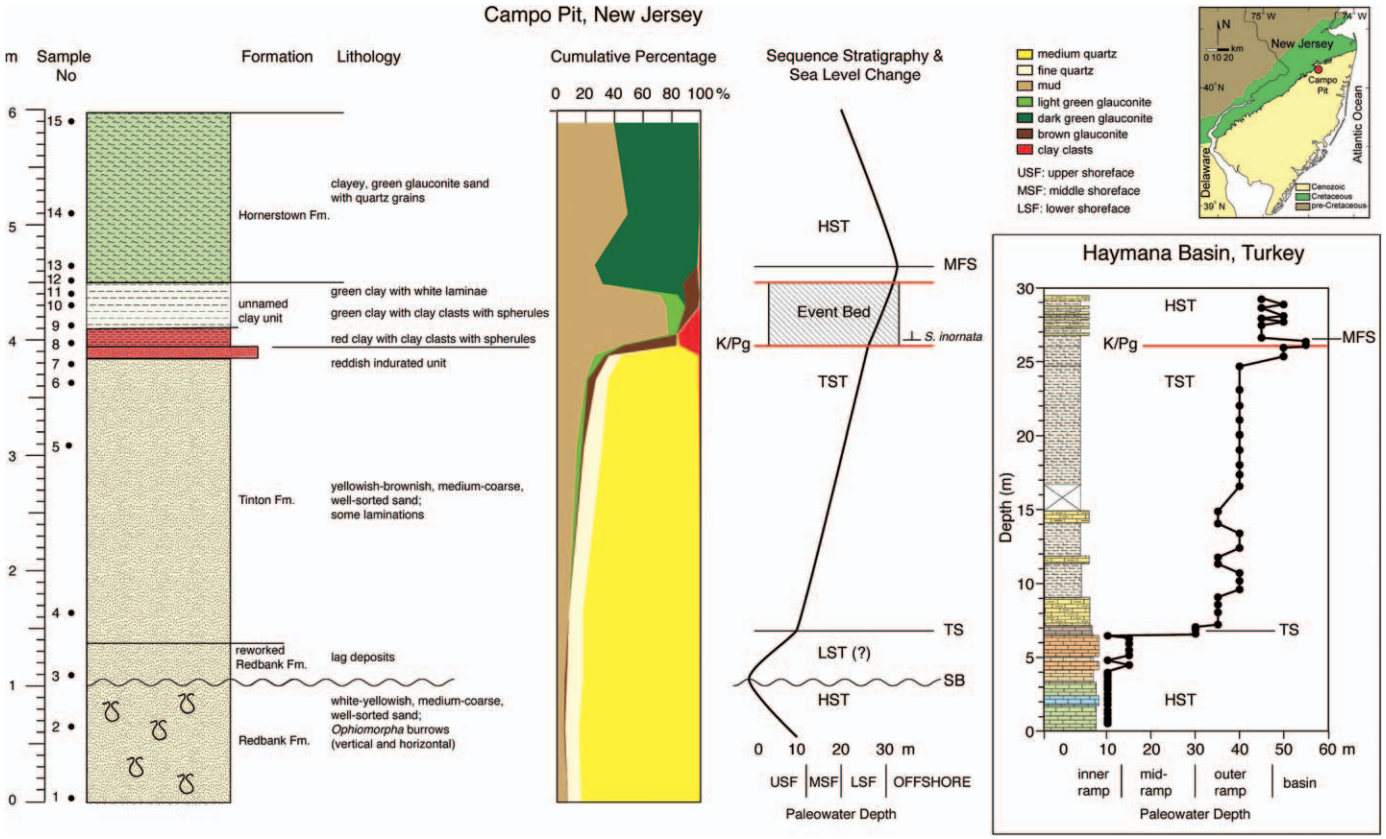

FIG. 11.—Lithostratigraphy, cumulative percentage diagram, and sequence stratigraphic interpretation of the Campo Pit section, New Jersey, USA and relative sea-level curve comparison of the section to Haymana Basin, Turkey. Constructions of the relative sea-level curves are explained in the text. Inset shows the geological map of New Jersey with the location of Campo Pit outcrop. Refer to the legend in Figure 2 for the Haymana Basin section. LST, lowstand systems tract; HST, highstand systems tract; TST, transgressive systems tract; SB, sequence boundary; TS, transgressive surface; MFS, maximum flooding surface.

to other criteria defining the boundary. The absence of the fecal-pellet horizon at Campo Pit (this study) and the adjacent Buck Pit core (Miller et al. 2010) suggests a facies control on this horizon due to nondeposition or post-depositional alteration in shoreface settings, and its presence in deeper-water environments (e.g., Haymana Basin (this study), deep New Jersey sections (Miller et al. 2010), and Swedish sections (Brotzen 1948)).

CONCLUSIONS

A section spanning the K/Pg boundary was examined in the Haymana Basin, Central Anatolia, Turkey, with detailed planktonic foraminiferal biostratigraphy, microfacies analysis, and sequence stratigraphy. The biostratigraphic record showed that the K/Pg boundary in the Haymana Basin is complete and the extinction of the planktonic foraminifera was abrupt and catastrophic, as has been shown by previous researchers in many other K/Pg sections globally. Zone P0 is characterized by the evolution of early Danian planktonic foraminifera and associated with an increase in clay minerals and echinoid fecal pellets; this increase seems to be a correlatable level to several New Jersey Coastal Plain sections. Our relative sea-level curve shows that the K/Pg boundary in the Haymana Basin was deposited during a sea-level rise below a MFS. Comparison of the section with the Campo Pit section, New Jersey, and other sections from Europe and North Africa showed a similar sea-level rise across the K/Pg boundary.

ACKNOWLEDGMENTS

We thank the Scientific Research Projects Coordination of the Middle East Technical University for providing financial support for this study. We would like to thank Mevlüt Ertan for his contribution to the improvement of the washing techniques, Zühtü Batı for reviews on the manuscript, Richard K. Olsson for discussions on the planktonic foraminiferal taxonomy and fecal pellets, James V. Browning for discussions on the Campo Pit section, and James D. Wright for comments. We are thankful to Brian Huber and Steve D'Hondt for reviews, and to Associate Editor Elias Samankassou and Editor Gene Rankey for comments.

REFERENCES

ADATTE, T., KELLER, G., AND STINNESBECK, W., 2002, Late Cretaceous to early Paleocene climate and sea-level fluctuations: the Tunisian record: Palaeogeography, Palaeoclimatology, Palaeoecology, v. 178, p. 165–196.

←

FIG. 10.—Photomicrographs of the microfacies types, clay minerals, and echinoid fecal pellets. **A)** Silty marl with planktonic and benthic foraminifera (MF9), sample no. A59. **B)** Silty marl with planktonic and benthic foraminifera (MF9), sample no. A55. **C)** Silty marl with clay minerals and fecal pellets (MF10), sample no. A51. **D)** Silty marl with clay minerals and fecal pellets (MF10), sample no. A51. **E)** Clay minerals just above the K/Pg boundary, sample no. A51. **F)** Clay minerals hand-picked from the washed sample, sample no. A51. **G)** Echinoid fecal pellet, sample no. A51. **H)** Echinoid fecal pellet hand-picked from the washed sample, sample no. A51. **I)** Scanning electron microscope image of an echinoid fecal pellet, sample no. A51. hb, hyaline benthic foraminifera; ab, agglutinated benthic foraminifera; p, planktonic foraminifera; q, quartz; c, clay minerals. Scale bar is 0.25 mm for A, B, C, D, E, and G and 100 μm for H and I.

Alegret, L., Molina, E., and Thomas, E., 2003, Benthic foraminiferal turnover across the Cretaceous/Paleogene boundary at Agost (southeastern Spain): paleoenvironmental inferences: Marine Micropaleontology, v. 48, p. 251–279.

Apellaniz, E., Baceta, J.I., Bernaola-Bilbao, G., Nunez-Betelu, K., Orue-Etxebarria, X., Payros, A., Pujalte, V., Robin, E., and Rocchia, R., 1997, Analysis of uppermost Cretaceous–lowermost Tertiary hemipelagic successions in the Basque Country (western Pyrenees): evidence for a sudden extinction of more than half planktic foraminifer species at the K/T boundary: Société Géologique de France Bulletin, v. 168, p. 783–793.

Arenillas, I., Arz, J.A., Grajales-Nishimura, J., Murillo-Muñetón, G., Alvarez, W., Camargo-Zanoguera, A., Molina, E., and Rosales-Domínguez, M., 2006, Chicxulub impact event is Cretaceous/Paleogene boundary in age: new micropaleontological evidence: Earth and Planetary Science Letters, v. 249, p. 241–257.

Ben Abdelkader, O., Ben Salem, H., Donze, P., Maamouri, A., Méon, H., Robin, É., Rocchia, R., and Froget, L., 1997, The K/T stratotype section of El Kef (Tunisia): events and biotic turnovers: Geobios, v. 21, p. 235–245.

Berggren, W.A., and Pearson, P., 2005, A revised tropical to subtropical Paleogene planktonic foraminiferal zonation: Journal of Foraminiferal Research, v. 35, p. 279–298.

Berggren, W.A., Kent, D.V., Swisher, C., III, and Aubry, M.-P., 1995, A revised Cenozoic geochronology and chronostratigraphy, *in* Berggren, W.A., Kent, D.V., Swisher, C.C., III, Aubry, M.-P., and Hardenbol, J., eds., Geochronology, Time Scales and Global Stratigraphic Correlation: SEPM, Special Publication 54, p. 129–212.

Bernaola, G., and Monechi, S., 2007, Calcareous nannofossil extinction and survivorship across the Cretaceous−Paleogene boundary at Walvis Ridge (ODP Hole 1262C, South Atlantic Ocean): Palaeogeography, Palaeoclimatology, Palaeoecology, v. 255, p. 132–156.

Brotzen, F., 1948, The Swedish Paleocene and Its Foraminiferal Fauna: Sweriges Geologiska Undersökning, v. 42, 140 p.

Browning, J.V., Miller, K.G., Sugarman, P.J., Kominz, M.A., McLaughlin, P.P., Jr, Kulpecz, A.A., and Feigenson, M.D., 2008, 100 Myr record of sequences, sedimentary facies and sea level change from Ocean Drilling Program onshore coreholes, US Mid-Atlantic coastal plain: Basin Research, v. 20, p. 227–248.

Burchette, T.P., and Wright, V.P., 1992, Carbonate ramp depositional systems, *in* Sellwood, B.W., eds., Ramps and Reefs: Sedimentary Geology, v. 79, p. 3–57.

Claeys, P., Kiessling, W., and Alvarez, W., 2002, Distribution of Chicxulub ejecta at the Cretaceous–Tertiary boundary, *in* Koeberl, C., and MacLeod, K.G., eds., Catastrophic Events and Mass Extinctions: Impacts and Beyond: Geological Society of America, Special Paper 356, p. 55–68.

Çiner, A., 1992, Sediméntologie et stratigraphie séquentielle du bassin d'Haymana à l'Eocene moyen Turquie: [PhD Thesis]: l'Universite Louis Pasteur, France, 190 p.

Çiner, A., Deynoux, M., Ricou, S., and Kosun, E., 1996, Cyclicity in the Middle Eocene Cayraz Carbonate Formation, Haymana Basin, Central Anatolia, Turkey: Palaeogeography, Palaeoclimatology, Palaeoecology, v. 121, p. 313–329.

Donovan, A.D., Baum, G.R., Blechschmidt, G.L., Loutit, T.S., Pflum, C.E., and Vail, P.R., 1988, Sequence stratigraphic setting of the Cretaceous–Tertiary boundary in central Alabama, *in* Wilgus, C.K., Kendall, C.G.S.C., Posamentier, H.W., and Ross, C.A., eds., Sea-Level Changes: An Integrated Approach: SEPM, Special Publication 42, p. 299–307.

Dunham, R.J., 1962, Classification of carbonate rocks according to the depositional texture, *in* Ham, W. E., ed., Classification of Carbonate Rocks: A Symposium: American Association of Petroleum Geologists, Memoir 1, p. 108–171.

El Gadi, M.S.M., and Brookfield, M.E., 1999, Open carbonate ramp facies, microfacies and paleoenvironments of the Gramame Formation (Maastrichtian), Pernambuco–Paraiba Basin, Northeastern Brazil: Journal of South American Earth Sciences, v. 12, p. 411–433.

Embry, A.F., and Klovan, J.E., 1971, A late Devonian reef tract on northeastern Banks Island: Northwest Territories: Bulletin of Canadian Petroleum Geology, v. 19, p. 730–781.

Emery, D., and Myers, K.J., 1996, Sequence Stratigraphy: Oxford, Blackwell Science, 297 p.

Flügel, E., 2004, Microfacies of Carbonate Rocks: Analysis, Interpretation and Application: Berlin, Springer, 976 p.

Fourquin, C., 1975, L'anatolie du Nord-Ouest, marge méridionale du continent europeén, histoire paléogéographique, tectonique et magmatique durant le Secondaire et Tertiare: Société Géologique de France, Bulletin, v. 7, p. 1058–1070.

Geel, T., 2000, Recognition of stratigraphic sequences in carbonate platform and slope deposits: empirical models based on microfacies analysis of Palaeogene deposits in southeastern Spain: Palaeogeography, Palaeoclimatology, Palaeoecology, v. 155, p. 211–238.

Georgescu, M.D., and Abramovich, S., 2008, A new serial Cretaceous planktic foraminifer (Family Heterohelicidae Cushman, 1927) from the Upper Maastrichtian of the equatorial Central Pacific: Journal of Micropalaeontology, v. 27, p. 117–123.

Görür, N., 1981, Tuzgölü-Haymana havzasının stratigrafik analizi: TJK, Iç Anadolunun Jeolojisi Simpozyumu, Ankara, v. 1, p. 60–66.

Görür, N., Oktay, Y.F., Seymen, I., and Şengör, A.M.C., 1984, Paleotectonic evolution of the Tuzgölü Basin complex, central Turkey: sedimentary record of the neo-tethyan closure, *in* Dixon, J., and Robertson, A.H.F., eds., The Geological Evolution of the Eastern Mediterranean: Geological Society of London, Special Publication 17, p. 467–481.

Haq, B., 2014, Cretaceous eustasy revisited: Global and Planetary Change, v. 113, p. 44–5.

Haq, B., Hardenbol, J., and Vail, P.R., 1987, Chronology of fluctuating sea levels since the Triassic: Science, v. 235, p. 1156–1167.

Heldt, M., Bachmann, M., and Lehmann, J., 2008, Microfacies, biostratigraphy, and geochemistry of the hemipelagic Barremian–Aptian in north-central Tunisia: influence of the OAE 1a on the southern Tethys margin: Palaeogeography, Palaeoclimatology, Palaeoecology, v. 261, p. 246–260.

Horowitz, A.S., and Potter, P.E., 1971, Introductory Petrography of Fossils: Berlin, Springer Verlag, 302 p.

Huber, B.T., 1991, 25. Maestrichtian Planktonic Foraminifer Biostratigraphy and the Cretaceous/Tertiary Boundary At Hole 738C (Kerguelen Plateau, Southern Indian Ocean), *in* Barron, J., and Larsen, B., eds., Proceedings of the Ocean Drilling Program, Scientific Results, v. 119, p. 451–465.

Huber, B.T., MacLeod, K.G., and Tur, N.A., 2008, Chronostratigraphic framework for upper Campanian–Maastrichtian sediments on the Blake Nose (subtropical North Atlantic): Journal of Foraminiferal Research, v. 38, p. 162–182.

Keller, G., 1988, Extinction, survivorship and evolution of planktic foraminifera across the Cretaceous/Tertiary boundary at El Kef, Tunisia: Marine Micropaleontology, v. 13, p. 239–263.

Keller, G., 2007, The Chicxulub impact and K-T mass extinction in Texas: South Texas Geological Society, Bulletin, v. XLVII, p. 15–44.

Keller, G., and Stinnesbeck, W., 1996, Sea-level changes, clastic deposits, and megatsunamis across the Cretaceous–Tertiary boundary, *in* MacLeod, N., and Keller, G., eds., Cretaceous–Tertiary Mass Extinctions: Biotic and Environmental Change: London, Norton, p. 415–449.

Knitter, H., 1979, Eine verbesserte Methode zur Gewinnung von Mikrofosilien aus harten, nicht schlammbaren Kalken: Geologische Blätter für Nordost-Bayern und angrenzende Gebiete: Erlangen, v. 29, p. 182–186.

Koçyiğit, A., 1991, An example of an accretionary forearc basin from Central Anatolia and its implications for the history of subduction of Neo-Tethys in Turkey: Geological Society of America, Bulletin, v. 103, p. 22–36.

Koçyiğit, A., and Lünel, T., 1987, Geology and tectonic setting of Alcı region, Ankara: Middle East Technical University, Journal of Pure and Applied Sciences, v. 20, p. 35–57.

Koçyiğit, A., Özkan, S., and Rojay, B., 1998, Examples of the forearc basin remnants at the active margin of northern Neo-Tethys: development and emplacement ages of the Anatolian Nappe, Turkey: Middle East Technical University Journal of Pure and Applied Sciences, v. 3, p. 183–210.

Kominz, M.A., Browning, J.V., Miller, K.G., Sugarman, P.J., Mizintseva, S., and Scotese, C., 2008, Late Cretaceous to Miocene sea-level estimates from the New Jersey and Delaware coastal plain coreholes: an error analysis: Basin Research, v. 20, p. 211–226.

Koutsoukos, E., 1996, Phenotypic experiments into new pelagic niches in early Danian planktonic foraminifera: aftermath of the K/T boundary event, *in* Hart, M.B., ed., Biotic Recovery from Mass Extinction Events: Geological Society of London, Special Publication 102, p. 319–335.

Li, L., and Keller, G., 1998, Maastrichtian climate, productivity and faunal turnovers in planktic foraminifera in South Atlantic DSDP sites 525A and 21: Marine Micropaleontology, v. 33, p. 55–86.

Lirer, F., 2000, A new technique for retrieving calcareous microfossils from lithified lime deposits: Micropaleontology, v. 46, p. 365–369.

Liu, C., and Olsson, R.K., 1992, Evolutionary radiation of microperforate planktonic Foraminifera following the K/T mass extinction event: Journal of Foraminiferal Research, v. 22, p. 328–346.

Luciani, V., 1997, Planktonic foraminiferal turnover across the Cretaceous–Tertiary boundary in the Vajont valley (Southern Alps, northern Italy): Cretaceous Research, v. 18, p. 799–821.

Luciani, V., 2002, High-resolution planktonic foraminiferal analysis from the Cretaceous–Tertiary boundary at Ain Settara (Tunisia): evidence of an extended mass extinction: Palaeogeography, Palaeoclimatology, Palaeoecology, v. 178, p. 299–319.

Luterbacher, P.H., and Premoli Silva, I., 1964, Biostratigrafia del limite cretaceo–terziario nell'Appennino centrale: Rivista Italiana di Paleontologia, v. 70, p. 67–117.

Miller, K.G., Sugarman, P.J., Browning, J.V., Kominz, M.A., Olsson, R.K., Feigenson, M.D., and Hernandez, J., 2004, Upper Cretaceous sequences and sea-level history, New Jersey coastal plain: Geological Society of America, Bulletin, v. 116, p. 368–393.

Miller, K.G., Kominz, M.A., Browning, J.V., Wright, J.D., Mountain, G.S., Katz, M.E., Sugarman, P.J., Cramer, B.S., Christie-Blick, N., and Pekar, S., 2005, The Phanerozoic record of global sea-level change: Science, v. 310, p. 1293–1298.

Miller, K.G., Sherrell, R., Browning, J.V., Field, M., Gallagher, W., Olsson, R.K., Sugarman, P.J., Tuorto, S., and Wahyudi, H., 2010, Relationship between mass extinction and iridium across the Cretaceous–Paleogene boundary in New Jersey: Geology, v. 38, p. 867–870.

Moucha, R., Forte, A.M., Mitrovica, J.X., Rowley, D.B., Quéré, S., Simmons, N.A., and Grand, S.P., 2008, Dynamic topography and long-term sea-level variations: There is no such thing as a stable continental platform: Earth and Planetary Science Letters, v. 271, p. 101–108.

Mount, J., 1985, Mixed siliciclastic and carbonate sediments: a proposed first-order textural and compositional classification: Sedimentology, v. 32, p. 435–442.

Müller, R.D., Sdrolias, M., Gaina, C., Steinberger, B., and Heine, C., 2008, Long-term sea-level fluctuations driven by ocean basin dynamics: Science, v. 319, p. 1357–1362.

Nederbragt, A.J., 1991, Late Cretaceous biostratigraphy and development of Heterohelicidae (planktic foraminifera): Micropaleontology, v. 37, p. 329–372.

Neumann, A.C., and Macintyre, I., 1985, Reef response to sea-level rise: keep-up, catch-up or give-up, *in* Fifth International Coral Reef Congress, Tahiti, Proceedings , v. 3, p. 105–110.

Obaidalla, N., 2005, Complete Cretaceous/Paleogene (K/P) boundary section at Wadi Nukhul, southwestern Sinai, Egypt: inference from planktic foraminiferal bio-stratigraphy: Revue de Paléobiologie, v. 24, p. 201–224.

Olsson, R.K., and Liu, C., 1993, Controversies on the placement of Cretaceous–Paleogene boundary and the K/P mass extinction of planktonic foraminifera: Palaios, v. 8, p. 127–139.

Olsson, R.K., Hemleben, C., Berggren, W.A., and Huber, B.T., eds., and Members of the Paleogene Planktonic Foraminifera Working Group, 1999, Atlas of Paleocene Planktonic Foraminifera: Smithsonian Contributions to Paleobiology, v. 85, 252 p.

Olsson, R.K., Miller, K.G., Browning, J.V., Wright, J.D., and Cramer, B.S., 2002, Sequence stratigraphy and sea-level change across the Cretaceous–Tertiary boundary on the New Jersey passive margin, *in* Koeberl, C., and MacLeod, K.G., eds., Catastrophic Events and Mass Extinctions: Impacts and Beyond: Geological Society of America, Special Paper 356, p. 97–108.

Özkan-Altiner, S., and Özcan, E., 1999, Upper Cretaceous planktonic foraminiferal biostratigraphy from NW Turkey: calibration of the stratigraphic ranges of larger benthonic foraminifera: Geological Journal, v. 34, p. 287–301.

Pardo, A., Ortiz, N., and Keller, G., 1996, Latest Maastrichtian and Cretaceous–Tertiary boundary foraminiferal turnover and environmental changes at Agost, Spain, *in* McLeod, N., and Keller, G., eds., Cretaceous–Tertiary Mass Extinctions: Biotic and Environmental Changes: New York, Norton, p.139–171.

Pardo, A., Adatte, T., Keller, G., and Oberhansli, H., 1999, Paleoenvironmental changes across the Cretaceous–Tertiary boundary at Koshak, Kazakhstan, based on planktic foraminifera and clay mineralogy: Palaeogeography, Palaeoclimatology, Palaeoecology, v. 154, p. 247–273.

Premoli Silva, I., and Verga, D., 2004, Practical Manual of Cretaceous Planktonic Foraminifera, *in* Verga, and Rettori, eds., International School on Planktonic Foraminifera, Course: Cretaceous: Universities of Perugia and Milan, Tipografia Pontefelcino, Perugia, 283 p.

Pujalte, V., 1998, Paleocene strata of the Basque Country, Western Pyrenees, northern Spain: facies and sequence development in a deep-water starved basin, *in* de Graciansky, P.C., Hardenbol, J., Jaquin, T., and Vail, P.R., eds., Mesozoic and Cenozoic Sequence Stratigraphy of European Basins: SEPM, Special Publication 60, p. 311–325.

Raup, D., and Sepkoski, J., Jr., 1982, Mass extinctions in the marine fossil record: Science, v. 215, p. 1501–1503.

Robaszynski, F., 1998, Planktonic foraminifera: Upper Cretaceous, Chart of Cretaceous biochronostratigraphy, *in* de Graciansky, P.C., Hardenbol, J., and Vail, P.R., eds., Mesozoic and Cenozoic Sequence Stratigraphy of European Basins: SEPM, Special Publication 60, 782 p.

Robaszynski, F., and Caron, M., 1995, Foraminifères planctoniques du Crétacé: commentaire de la zonation Europe–Méditerranée: Société Géologique de France, Bulletin, v. 166, p. 681–692.

Robaszynski, F., Caron, M., Donoso Gonzalez, M.J., Wonders, A.H., and The European Working Group on Planktonic Foraminifera, 1984, Atlas of Late Cretaceous Globotruncanids: Revue de Micropaléontologie, v. 26, p. 145–305.

Scholle, P.A., and Ulmer-Scholle, D.S., 2003, A Color Guide to the Petrography of Carbonates Rocks: Grains, Textures, Porosity, Diagenesis: American Association of Petroleum Geologists, Memoir 77, 474 p.

Schulte, P., Alegret, L., Arenillas, I., Arz, J.A., Barton, P., Bown, P., Bralower, T.J., Christeson, G., Claeys, P., and Cockell, C., 2010, The Chicxulub asteroid impact and mass extinction at the Cretaceous–Paleogene boundary: Science, v. 327, p. 1214–1218.

Smit, J., 1982, Extinction and evolution of planktonic foraminifera after a major impact at the Cretaceous/Tertiary boundary, *in* Silver, L.T., and Schultz, P.H., eds., Geological Implications of Impacts of Large Asteroid and Comets on the Earth: Geological Society of America, Special Paper 190, p. 329–352.

Smit, J., 1999, The global stratigraphy of the Cretaceous–Tertiary boundary impact ejecta: Annual Review of Earth and Planetary Sciences, v. 27, p. 75–113.

Şengör, A.M.C., and Yilmaz, Y., 1981, Tethyan evolution of Turkey: a plate tectonic approach: Tectonophysics, v. 75, p. 181–241.

Ünalan, G., Yüksel, V., Tekeli, T., Gönenç, O., Seyirt, Z., and Hüseyin, S., 1976, Haymana-Polatlı yöresinin (Güneybatı Ankara) Üst Kretase-Alt Tersiyer stratigrafisi ve paleogeografik evrimi: TJK Bülteni, v. 19, p. 159–176.

Vail, P.R., Mitchum, R.M., Jr., and Thompson, S., III, 1977, Seismic stratigraphy and global changes of sea level: Part 3. Relative changes of sea level from coastal onlap. *in* Payton, C.E., ed., Seismic Stratigraphy Applications to Hydrocarbon Exploration: American Association of Petroleum Geologists, Memoir 26, p. 63–81.

Voigt, E., 1929, Die Lithogenese der Flach- und Tiefwassersedimente des jüngeren Oberkreidemeeres: Halle, Hallescher Verband zur Erforschung der mitteldeutschen Bodenschätze und Verwertung, Jahrbuch, v. 8, 136 p.

Wade, B.S., Pearson, P., Berggren, W.A., and Palike, H., 2011, Review and revision of Cenozoic tropical planktonic foraminiferal biostratigraphy and calibration to the geomagnetic polarity and astronomical time scale: Earth-Science Reviews, v. 104, p. 111–142.

Wilson, J.L., 1975, Carbonate Facies in Geologic History: New York, Springer-Verlag, 469 p.

Yüksel, S., 1970, Etude géologique de la region d'Haymana (Turquie Centrale) [Thèse]: Faculte des Sciences, L'Université de Nancy, 179 p.

Received 24 October 2013; accepted 6 February 2015.